Quantum statistical theory of fluorescence of low density Frenkel excitons in a crystal slab

Chang-qi Cao*
CCAST(World Lab), P.O. Box 8730, Beijing 10080, China

Hui Cao†
Department of Physics and Astronomy, Northwestern University, Evanston, Illinois 60208-3112

Yi-xi Liu‡
Institute of Theoretical Physics, Academia Sinica, Beijing 100080, China

(Received 22 November 1999; revised manuscript received 18 May 2000)

The fluorescence of Frenkel excitons in low density regime is studied without the aid of rotating wave approximation and Markov approximation. The evolution of the emitted field is derived in terms of its initial conditions. It is found that the usual interaction Hamiltonian of $(e/mc)\mathbf{P}\cdot\mathbf{A}$ type leads to unreasonable characteristic equation for decay rates. Only when the term $(e^2/2mc^2)\mathbf{A}^2$ is added to the $(e/mc)\mathbf{P}\cdot\mathbf{A}$, the result becomes reasonable. The case of single lattice layer is studied in detail. Different features of statistical properties of the superfluorescence are shown as compared with that of atom aggregate. Double and triple lattice-layer cases are also studied to show the effect of coupling between the excitons of different wave vectors.

I. INTRODUCTION

The spontaneous emission of low density excitons (Wannier or Frenkel) is of collective character even if there is only one exciton. The reason is that each exciton migrates over the whole quantum well (or crystal slab) coherently when the exciton density is low (so that overlapping can be neglected), leading to a collective transition dipole moment to interact with the electromagnetic field. But the fluorescence of such an exciton may have different features as compared with the usual superfluorescence of fully population-inverted atom aggregate. In the latter case the atoms radiate independently with each other in the initial stage, they become cooperative only after a time decay, resulting in an intense pulse of peak shape. The emitted field will show different statistical properties in the initial stage and later on stages. We shall see that the fluorescence of low density excitons are quite different. In general the exciton may have many eigenmodes. For those eigenmodes which are phase matching or nearby matching with the emitted light, the exciton fluorescence is superradiant, and this superfluorescence will exhibit identical statistical character during the whole process as will be demonstrated in this paper.

Another different feature between superfluorescences of excitons and of atom aggregate lies in that the cooperation of atom aggregate is limited by a finite length, the so called cooperation length[1] since the atoms come into phase coherently correlated state through the radiation field itself which has a finite extent, while the exciton of low density is a coherent excitation over the whole crystal, provided the carrier quantum well or crystal slab is ideal (no trapping effect occurs). For Wannier exciton, this feature is obvious since it is a pair of free electron and free hole bound together, still movable freely as a whole. Frenkel exciton is usually an excitation of lattice atom (molecular) in the crystal. However, the excitation will not be located at a fixed lattice, but transfer from one lattice to another due to atom-atom interaction, so that the stationary state is also a phase coherently superposed excited state over all the lattice.[2] This feature is reflected in the proportionality of exciton-photon coupling constant G to $\sqrt{N_T}$ in low density regime, where N_T is the total number of atoms in the crystal. Nevertheless, this does not mean that the superradiant rate Γ will tend to infinity as $N_T \rightarrow \infty$. The value of Γ will be limited by two effects: one is the reduction of the available photon states which restrains the value of Γ for large lateral crystal extension, another is the reabsorption of the emitted photon, which restrains Γ for large longitudinal crystal extension. The first effect will be demonstrated in Sec. V, the second effect is related to the formation of a new stationary state, polariton, as longitudinal extension tens to infinity.

In the literature[3–8] the authors usually devote themselves to deduce the radiant rate Γ. The simplest way to this aim is to calculate Γ by the perturbation theory, namely in terms of Fermi golden rule. This approach has ignored reabsorption and stimulation effect so that it cannot be applied to thick crystal slab. Hanamura presented a different approach, he deduced a characteristic equation for Γ for the superfluorescence of Wannier excitons[3] in a two-dimensional quantum well with thickness of exciton diameter. But his characteristic equation, as we will see later, suffers the problem of existing a superfluous unphysical root which will lead to unreasonable temporal evolution of the field. Knoester proposed a general formulation for fluorescence of Frenkel excitons[5] and gave a correct characteristic equation for the $N=1$ case, which is free from the above-mentioned unphysical pole. He also studied the crossover from the superradiant excitons to bulk polaritons. However, no detailed derivation is given for the effective coupling function $F_{kk'}(\omega)$ and for the character equation therein. Actually these results in Ref. 5 cannot be derived from simple coupling of form $(e/mc)\mathbf{P}\cdot\mathbf{A}$, as will be seen in the following paragraphs.

In addition, one cannot limit oneself just to deriving the radiant rate. The photon field operator (and exciton field op-

0163-1829/2000/62(24)/16453(21)/$15.00 PRB 62

erator) also deserves investigation. It not only exhibits the dynamics of the radiation process, but also allows people to study the statistical properties of the emitted light. We note that no such statistical properties were investigated in Hanamura's paper[3] and Knoester's paper.[5]

Bjork *et al.*[7] have studied the time evolution of radiation intensity based upon the work of Rehler and Eberly,[9] in which each atom is assumed in a pure state and the time variation of the total atomic energy $W(t)$ is derived by a relation which connects $W(t)$ and radiation power $I(t)$. Thus their results could not give any information with regard to the statistical properties of the emitted light field. Moreover, the stimulated emission and absorption are also neglected in their treatment.

Tobihiro *et al.* have investigated the superfluorescence of a highly excited linear mesoscopic chain of moleculars.[10,11] They even take the static dipole-dipole interaction into account. But still no statistical properties of emitted light are reported.

In this paper, we shall limit to the case of low exciton regime and also to the case in which the wave vectors of excitons are perpendicular to the crystal slab. In this case, only the light modes propagating perpendicular to the crystal slab need be taken into account, and hence the coupled Heisenberg equations for exciton-photon system can be solved without Born-Markov as well as rotating wave approximation.

In Sec. II, we present the basic formulation with interaction Hamiltonian of $(e/mc)\mathbf{P}\cdot\mathbf{A}$ type which is usually adopted in studying radiation problem. A closed expression of the function $F_{kk'}(\omega)$ which measures the coupling of excitons with different wave vectors mediated by photons is derived for arbitrary number of lattice layers N. One sees that Eq. (1) of Ref. 5 is of the same form with our result, but the function $F_{kk'}$ is different from that in our derivation, apart a phase factor, by a substantial factor ω/Ω.

In Sec. III, the result obtained in the Sec. II is analyzed in the case of single lattice layer. We find that a root of the characteristic equation lies in the upper half of complex ω plane, which corresponds to negative value of Γ and hence leads to unphysical evolution of field operators. Change to the interaction of $-\mathbf{E}\cdot\mathbf{d}$ type, another problem emerges instead: a large real term appears in the characteristic equation which also makes its root unreasonable. Section IV deals with interaction Hamiltonian with $(e^2/2mc^2)\mathbf{A}^2$ term added to the $(e/mc)\mathbf{P}\cdot\mathbf{A}$. A modified reduced dynamical equation for exciton operator is obtained.

In Sec. V the single lattice-layer case is examined in detail on the basis of the modified reduced dynamical equation given in Sec. IV. The characteristic equation now becomes reasonable. The evolution of electric field is derived in terms of initial state of exciton. The superradiance character of the fluorescence in this case is analyzed, with the reduction factor due to photon states contraction derived explicitly. The light intensity as well as the first- and second-order degree of coherence are calculated to show the new features of the exciton fluorescence. Some striking results concerning the light intensity and degrees of coherence are presented. Section VI deals the cases of double lattice layers and triple lattice layers. The coupling between excitons with different wave vectors is taken into account. We see that only one mode is superradiant. Section VII presents a brief summary.

II. BASIC FORMULATION WITH P·A COUPLING

As mentioned in Sec. I, we consider a simple model of fluorescence of Frenkel excitons in a plane crystal slab which has ideal cubic lattice with N layers. The wave vectors of the excitons and light fields are all assumed perpendicular to the slab. The density of excitons is assumed low, so that the space filling effect and exciton-exciton direct coupling terms[12] can be neglected. This model is similar to that of Ref. 3 and should be the same as adopted by Ref. 5.

For $(e/mc)\mathbf{P}\cdot\mathbf{A}$ coupling, the $\hat{H}_{int}$ between the photon and lattice atoms (two level) is of the form

$$\hat{H}_{int}(t)=\hbar\sum_{q;l;j} g(q)\hat{b}^{\dagger}_{lj}(t)[\hat{a}_q(t)e^{iqla}+\hat{a}^{\dagger}_q(t)e^{-iqla}]+\text{H.c.},\tag{1}$$

where $\hat{a}_q$ and $\hat{a}^{\dagger}_q$ are the annihilation and creation operators of the photon with wave vector q, respectively, $\hat{b}_{lj}$ and $\hat{b}^{\dagger}_{lj}$ denote the creation and annihilation operator for an excitation of the two-level atom at jth lattice site in the lth layer. a denotes the lattice constant. The effective atom-photon coupling constant $g(q)$ is taken as real with the expression

$$g(q)=\sqrt{\frac{2\pi\Omega^2}{V\hbar|q|c}}d,\tag{2}$$

where Ω denotes the electronic transition frequency of the isolated lattice atom, d represents its transition dipole moment, which is assumed real and its direction lying in the slab plane. V is the normalization volume for the photon. Note that no rotating wave approximation is made in Eq. (1). In the low density excitation region $\hat{b}_{lj}$ and $\hat{b}^{\dagger}_{lj}$ are bosonic operators, satisfying the commutation relation

$$[\hat{b}_{lj}(t),\hat{b}^{\dagger}_{l'j'}(t)]=\delta_{ll'}\delta_{jj'}\,.\tag{3}$$

Define the collective operator for the lth layer as

$$\hat{B}^{\dagger}_l(t)=\frac{1}{\sqrt{N_L}}\sum_j\ \hat{b}^{\dagger}_{lj}(t),\quad \hat{B}_l(t)=\frac{1}{\sqrt{N_L}}\sum_j\ \hat{b}_{lj}(t),\tag{4}$$

where N_L is the total lattices sites within each layer. Evidently we have

$$[\hat{B}_l(t),\hat{B}^{\dagger}_{l'}(t)]=\delta_{ll'}\,.$$

Equation (1) may be rewritten as

$$\hat{H}_{int}(t)=\sum_{q,l}\ \sqrt{N_L}g(q)\hat{B}^{\dagger}_l(t)[\hat{a}_q(t)+\hat{a}^{\dagger}_{-q}(t)]e^{iqla}+\text{H.c.};\tag{5}$$

no static dipole moment is taken into account for simplicity.

Transform to Frenkel exciton annihilation operator with wave vector k,

$$\hat{B}_k(t)=\frac{1}{\sqrt{N}}\sum_l\ e^{-ikla}\hat{B}_l(t),\tag{6}$$

where N is the total number of layers, and

$$k=\frac{2\pi m}{Na}, \tag{7a}$$

in which m's are taken as symmetrical to zero:

$$m=-\tfrac{1}{2}(N-1),-\tfrac{1}{2}(N-3),\ldots,\tfrac{1}{2}(N-1), \tag{7b}$$

since the values of k are assumed such that to each k there is a corresponding $-k$. The values of l in Eq. (6) will be the same as m. It is easy to show that the exciton operators satisfy the following bosonic commutation relation

$$[\hat{B}_k(t),\hat{B}_{k'}(t)]=\delta_{k,k'}. \tag{8}$$

We get therefore the interaction Hamiltonian between the Frenkel excitons and photons as

$$\hat{H}_{int}=\hbar\sum_{q,k} G(q)O(k+q)[\hat{B}_k(t)+\hat{B}^\dagger_{-k}(t)][\hat{a}_q(t)+\hat{a}^\dagger_{-q}(t)] \tag{9}$$

in which

$$O(k+q)=\frac{1}{N}\sum_{l=-(1/2)(N-1)}^{(1/2)(N-1)} e^{i(k+q)la}=\frac{1}{N}\frac{\sin\frac{1}{2}N(k+q)a}{\sin\frac{1}{2}(k+q)a}, \tag{10a}$$

$$G^2(q)=N_T g^2(q)=N_T\frac{2\pi\Omega^2}{V\hbar|q|c}d^2, \tag{10b}$$

where $N_T=NN_L$, representing the total number of lattice sites within the crystal slab as mentioned in Sec. I. $O(k+q)$ may be called as wave-vector matching factor [notice that our $O(k+q)$ is defined somewhat differently from that in Ref. 5, apart from a phase factor $e^{-(1/2)i(k+q)(N+1)a}$, by a factor $1/\sqrt{N}$]. In our definition, it is real and equals to 1 for $k+q=0$, and $O(k+q)<1$, for $k+q\neq 0$.

It is well known that the exciton in a bulk crystal does not radiate, but forms polariton instead. This shows that a general treatment of exciton radiation should take the reabsorption effect into account, and one should calculate the radiant rate by solving dynamical equation[3,5] not simply by utilizing Fermi golden rule.

The Heisenberg equations for exciton and photon operators can be easily got from $\hat{H}_{int}(t)$, with the results

$$i\frac{\partial}{\partial t}\hat{a}_q(t)=|q|c\hat{a}_q(t)+G(q)\sum_k O(k-q)[\hat{B}_k(t)+\hat{B}^\dagger_{-k}(t)], \tag{11a}$$

$$i\frac{\partial}{\partial t}\hat{a}^\dagger_{-q}(t)=-|q|c\hat{a}^\dagger_{-q}(t)-G(q)\sum_k O(k-q)\times[\hat{B}_k(t)+\hat{B}^\dagger_{-k}(t)], \tag{11b}$$

$$i\frac{\partial}{\partial t}\hat{B}_k(t)=\Omega\hat{B}_k(t)+\sum_q G(q)O(q-k)[\hat{a}_q(t)+\hat{a}^\dagger_{-q}(t)], \tag{11c}$$

$$i\frac{\partial}{\partial t}\hat{B}^\dagger_{-k}(t)=-\Omega\hat{B}^\dagger_{-k}(t)-\sum_q G(q)O(q-k)\times[\hat{a}_q(t)+\hat{a}^\dagger_{-q}(t)]. \tag{11d}$$

Define the half side Fourier transformation as

$$\hat{a}_q(\omega)=\int_0^\infty \hat{a}_q(t)e^{i\omega t}dt, \tag{12a}$$

$$\hat{a}^\dagger_{-q}(\omega)=\int_0^\infty \hat{a}^\dagger_{-q}(t)e^{i\omega t}dt, \tag{12b}$$

and the similar for $\hat{B}_k(\omega)$ and $\hat{B}^\dagger_{-k}(\omega)$ [note that $\hat{a}^\dagger_{-q}(\omega)=\hat{a}_{-q}(-\omega)^\dagger$], Eqs. (11) are then transformed to the algebraic equations

$$(\omega-|q|c)\hat{a}_q(\omega)=G(q)\sum_k O(k-q)[\hat{B}_k(\omega)+\hat{B}^\dagger_{-k}(\omega)]+i\hat{a}_q(0), \tag{13a}$$

$$(\omega+|q|c)\hat{a}^\dagger_{-q}(\omega)=-G(q)\sum_k O(k-q)[\hat{B}_k(\omega)+\hat{B}^\dagger_{-k}(\omega)]+i\hat{a}_{-q}(0), \tag{13b}$$

$$(\omega-\Omega)\hat{B}_k(\omega)=\sum_q G(q)O(q-k)[\hat{a}_q(\omega)+\hat{a}^\dagger_{-q}(\omega)]+i\hat{B}_k(0), \tag{13c}$$

$$(\omega+\Omega)\hat{B}^\dagger_{-k}(\omega)=-\sum_q G(q)O(q-k)[\hat{a}_q(\omega)+\hat{a}^\dagger_{-q}(\omega)]+i\hat{B}^\dagger_{-k}(0), \tag{13d}$$

in which $\hat{a}_q(0)$ and $\hat{B}_k(0)$ means $\hat{a}_q(t)|_{t=0}$ and $\hat{B}_k(t)|_{t=0}$, etc.

To ensure convergence, the ω in Eqs. (12) is actually attached to an infinitesimal positive imaginary part ϵ, namely ω stands for $\omega+i\epsilon$. The inverse transformation of Eqs. (12) is readily seen to be

$$\hat{a}_q(t)=\frac{1}{2\pi}\int_{-\infty+i\epsilon}^{\infty+i\epsilon}\hat{a}_q(\omega)e^{-i\omega t}d\omega,$$

$$\hat{a}^\dagger_{-q}(t)=\frac{1}{2\pi}\int_{-\infty+i\epsilon}^{\infty+i\epsilon}\hat{a}^\dagger_{-q}(\omega)e^{-i\omega t}d\omega. \tag{14}$$

From Eqs. (13a) and (13b), one gets

$$(\omega^2-q^2c^2)[\hat{a}_q(\omega)+\hat{a}^\dagger_{-q}(\omega)]=2|q|cG(q)\sum_k O(k-q)\times[\hat{B}_k(\omega)+\hat{B}^\dagger_{-k}(\omega)]+i[(\omega+|q|c)\hat{a}_q(0)+(\omega-|q|c)\hat{a}^\dagger_{-q}(0)]. \tag{15}$$

Substituting Eq. (15) into Eq. (13c) yields

$$(\omega-\Omega)\hat{B}_k(\omega)=\sum_{k'} F_{kk'}(\omega)[\hat{B}_{k'}(\omega)+\hat{B}^{\dagger}_{-k'}(\omega)] + \sum_q G(q)O(q-k) \times\left[\frac{1}{\omega-|q|c}\hat{a}_q(0)+\frac{1}{\omega+|q|c}\right]+i\hat{B}_k(0) \tag{16}$$

in which

$$F_{kk'}(\omega)=\sum_q \frac{2|q|cG^2(q)O(k-q)O(q-k')}{\omega^2-q^2c^2} \tag{17}$$

measuring the coupling of excitons with different wave vectors mediated by photons of various q. We take the photon normalization volume V to be AL where A is the area of the crystal slab, and let the slab located at the middle of the volume. When L is sufficient large, the summation in Eq. (17) may be converted to integration to give

$$F_{kk'}(\omega)=-\frac{Na\Omega f^2}{4\pi c^2}\int_{-\infty}^{+\infty}dq\,\frac{O(k-q)O(q-k')}{q^2-\dfrac{\omega^2}{c^2}}, \tag{18}$$

where

$$f^2=\frac{8\pi\Omega d^2}{\hbar a^3}, \tag{19}$$

a coupling parameter which is independent of photon momentum and photon normalization volume. Its dimension is the same as $G^2(q)$.

For comparing Eq. (16) with Eqs. (1) and (2) of Ref. 5, we momentarily neglect the terms proportional to $\hat{a}_q(0)$ and $\hat{a}^{\dagger}_{-q}(0)$ in the former and let $J=0$ in the latter. After this abridgement, these two equations have the same form. But actually they are different, because our $F_{kk'}(\omega)$ differs from Eq. (2) of Ref. 5, apart from a phase factor, by a substantial factor Ω/ω. We note that the coupling in Ref. 5 is also taken as $P\cdot A$ type.

Knoester further proposed[5] that $F_{kk'}(\omega)$ is strongly peaked around $k=k'$ and may be taken as $F_{kk}(\omega)\delta_{kk'}$ to a good approximation. This proposition of course holds exactly for $N=1$ and $N=\infty$, since for $N=1$ there is only one value of k namely $k=0$ and for $N=\infty$ it corresponds to conservation of k. It may possibly be a good approximation when N is large but will not be valid in general, as already doubted by Andreani,[13] and also will be seen directly in Sec. VI. Thus a closed expression of $F_{kk'}(\omega)$ for $k\neq k'$ is desirable.

Substituting Eq. (10a) into Eq. (18), and carrying out the integration, we get

$$F_{kk'}(\omega)=-\frac{af^2\Omega}{8Nc\omega}\left[\frac{\sin\frac{1}{2}\left(k'+\frac{\omega}{c}\right)Na}{\sin\frac{1}{2}\left(k'+\frac{\omega}{c}\right)a}\,\frac{e^{(i/2)(k+\omega/c)Na}}{\sin\frac{1}{2}\left(k+\frac{\omega}{c}\right)a} - \frac{\sin\frac{1}{2}\left(k'-\frac{\omega}{c}\right)Na}{\sin\frac{1}{2}\left(k'-\frac{\omega}{c}\right)a}\,\frac{e^{-(i/2)(k-\omega/c)Na}}{\sin\frac{1}{2}\left(k-\frac{\omega}{c}\right)a} + \frac{\sin\frac{1}{2}(k-k')Na}{\sin\frac{1}{2}(k-k')a} \times\frac{\sin\frac{\omega}{c}a}{\left[\sin\frac{1}{2}\left(k+\frac{\omega}{c}\right)a\right]\left[\sin\frac{1}{2}\left(k-\frac{\omega}{c}\right)a\right]}\right]. \tag{20}$$

for the details, see Appendix A. When $N\rightarrow\infty$, the first two terms tend to zero,[5] hence

$$\lim_{N\rightarrow\infty}F_{kk'}(\omega) =-\frac{af^2\Omega}{8c\omega}\,\frac{\sin\frac{\omega}{c}a}{\left[\sin\frac{1}{2}\left(k+\frac{\omega}{c}\right)a\right]\left[\sin\frac{1}{2}\left(k-\frac{\omega}{c}\right)a\right]}\,\delta_{kk'}, \tag{21}$$

consistent with the conservation of k.

To deduce $\hat{a}_q(\omega)$, we need first to evaluate $\hat{B}_k(\omega)+\hat{B}^{\dagger}_{-k}(\omega)$. From Eq. (16) and its Hermitian conjugate, we get a closed equation for $\hat{B}_k(\omega)+\hat{B}^{\dagger}_{-k}(\omega)$ as follows:

$$\sum_{k'}[(\omega^2-\Omega^2)\delta_{kk'}-2\Omega F_{kk'}(\omega)][\hat{B}_{k'}(\omega)+\hat{B}^{\dagger}_{-k'}(\omega)] =i[(\omega+\Omega)\hat{B}_k(0)+(\omega-\Omega)\hat{B}^{\dagger}_{-k}(0)] +2i\Omega\sum_q G(q)O(q-k) \times\left[\frac{1}{\omega-|q|c}\hat{a}_q(0)+\frac{1}{\omega+|q|c}\hat{a}^{\dagger}_{-q}(0)\right]. \tag{22}$$

This is what we call reduced dynamical equation for exciton operator in Sec. I. Having the expression of $F_{kk'}(\omega)$, in principle this equation may be solved for $\hat{B}_k(\omega)+\hat{B}^{\dagger}_{-k}(\omega)$ for arbitrary N. Substituting the result of $\hat{B}_k(\omega)+\hat{B}^{\dagger}_{-k}(\omega)$ into Eqs. (13a) and (13b) to get $\hat{a}_q(\omega)$ and $\hat{a}^{\dagger}_{-q}(\omega)$, the time evolution of photon field operator is then derived by the inverse Fourier transformation

$$\hat{E}(z,t)=\frac{1}{2\pi}\int_{-\infty+i\epsilon}^{\infty+i\epsilon}\hat{E}(z,\omega)e^{-i\omega t}d\omega, \tag{23}$$

where the z axis is taken perpendicular to the crystal slab surface, and $\hat{E}(z,\omega)$ is given by

$$\hat{E}(z,\omega)=i\sum_{q}\sqrt{\frac{2\pi|q|c\hbar}{V}}[\hat{a}_{q}(\omega)-\hat{a}^{\dagger}_{-q}(\omega)]e^{iqz}$$
$$=i\int_{-\infty}^{+\infty}\sqrt{\frac{|q|c\hbar L}{2\pi A}}[\hat{a}_{q}(\omega)-\hat{a}^{\dagger}_{-q}(\omega)]e^{iqz}dq \tag{24}$$

for sufficient large L.

III. THE PROBLEM FOR P·A COUPLING

Although the $(e/mc)\mathbf{P}\cdot\mathbf{A}$ interaction Hamiltonian is commonly used in treating emission and absorption problem, we find a serious problem in the above formulation. Let us see the simplest case, $N=1$. Now the only allowable value of k is zero. As mentioned in Appendix A, when $N=1$ the integral on the right-hand side of Eq. (18) is just equal to $\pi ic/\omega$, hence

$$F_{00}(\omega)=-i\frac{af^{2}\Omega}{4c\omega}=-i\frac{\Omega\eta}{2\omega} \tag{25}$$

with

$$\eta=\frac{af^{2}}{2c}. \tag{26}$$

After neglecting the terms proportional to $\hat{a}_{q}(0)$ and $\hat{a}^{\dagger}_{-q}(0)$ as did in Ref. 5, Eq. (22) is reduced to

$$\hat{B}_{0}(\omega)+\hat{B}_{0}^{\dagger}(\omega)=\frac{i}{\omega^{2}-\Omega^{2}+i\eta\dfrac{\Omega^{2}}{\omega}}[(\omega+\Omega)\hat{B}_{0}(0)+(\omega-\Omega)\hat{B}_{0}^{\dagger}(0)]. \tag{27}$$

The roots of the characteristic equation

$$\omega^{2}-\Omega^{2}+i\eta\frac{\Omega^{2}}{\omega}=0 \tag{28}$$

will determine the poles of $\hat{B}_{0}(\omega)+\hat{B}_{0}^{\dagger}(\omega)$ which turn out to be the decay rates and frequency shifts of the excitons. The above characteristic equation is a third-order algebraic equation:

$$\omega^{3}-\Omega^{2}\omega+i\eta\Omega^{2}=0. \tag{29}$$

Since $\eta/\Omega\ll1$, the roots of Eq. (29) are given approximately by

$$\omega_{1,2,3}\cong\Omega-\tfrac{1}{2}i\eta,\quad -\Omega-\tfrac{1}{2}i\eta,\quad i\eta. \tag{30}$$

The root $\omega_{3}\cong i\eta$ in the upper half ω plane is an unphysical pole of $\hat{B}_{0}(\omega)+\hat{B}_{0}^{\dagger}(\omega)$. When we use Eqs. (27) and (13a) and (13b) to evaluate $\hat{E}(z,t)$ according to Eqs. (25) and (26), the result will contain an unphysical term contributed by the root ω_{3}, which gives $\langle\hat{E}(z,t)\rangle\neq0$ for spacelike internal $|z|>ct$ (see Sec. V). Changing the integration path of ω to line $-\infty+i(\eta+\epsilon)\rightarrow+\infty+i(\eta+\epsilon)$ may eliminate this problem but another problem arises: there will be a growing term $\sim e^{\eta t}$. Both results are unacceptable.

We note that even if we remove a factor Ω/ω from right-hand side of Eq. (25) to make our $F_{00}(\omega)$ coincide with that of Knoester, the characteristic equation is still different from Eq. (3) of Ref. 5 and remains to give unphysical root. In addition, we note that the Eq. (12) of Ref. 3 for zero transverse wave vector is the same as our Eq. (29), hence it also suffers from the problem of existing an unphysical root. Change to $-\mathbf{E}\cdot\mathbf{d}$ coupling, the only alteration is $G^{2}(q)$ being modified to $N_{T}(2\pi|q|c/V\hbar)d^{2}$, so the function $F_{00}(\omega)$ for $N=1$ becomes, instead of Eq. (25),

$$F_{00}(\omega)=-\eta\frac{c}{2\pi\Omega}\int_{-\infty}^{+\infty}dq\,\frac{q^{2}}{q^{2}-\dfrac{\omega^{2}}{c^{2}}}. \tag{31}$$

Writing the integrand as $1+(\omega^{2}/c^{2})[1/(q^{2}-\omega^{2}/c^{2})]$ and remembering that ω has an infinitesimal positive imaginary part, the second term can be easily integrated out, resulting in

$$F_{00}(\omega)=-i\eta\frac{\omega}{\Omega}-\eta\frac{c}{2\pi\Omega}\int_{-\infty}^{+\infty}dq. \tag{32}$$

The real part of the above $F_{00}(\omega)$ now tends to minus infinity. Even if we cut off the integration range at $q_{M}\sim1/a$ on account of our dipole approximation, $(-2\Omega\,\mathrm{Re}\,F_{00})$ is still of order $8d^{2}\Omega/\hbar a^{3}\sim8e^{2}\Omega/\hbar a$. Such large value of $(-2\Omega\,\mathrm{Re}\,F_{00})$ will make the characteristic equation

$$\omega^{2}+i\eta\omega-\Omega^{2}-2\Omega\,\mathrm{Re}\,F_{00}=0 \tag{33}$$

unreasonable, since its roots should have zero real parts, which means the eigenfrequency drops down to zero.

IV. THE FORMULATION WITH P·A PLUS A^2 COUPLING

It is seen from last section that $e/mc\mathbf{P}\cdot\mathbf{A}$ coupling leads to unphysical result and $-\mathbf{E}\cdot\mathbf{d}$ coupling also results in unreasonable characteristic equation. We remind that a two-photon coupling term $(e^{2}/2mc^{2})\mathbf{A}^{2}$ has been neglected in the $(e/mc)\mathbf{P}\cdot\mathbf{A}$ formulation. Now this term will be taken into account, which changes Eq. (9) to

$$\hat{H}_{int}(t)=\hbar\sum_{q,k}G(q)O(k+q)[\hat{B}_{k}(t)+\hat{B}^{\dagger}_{-k}(t)]\times[\hat{a}_{q}(t)+\hat{a}_{-q}(t)]+\hbar\sum_{q,q',l}f(q,q')\times[\hat{a}_{q}(t)+\hat{a}^{\dagger}_{-q}(t)][\hat{a}_{q'}(t)+\hat{a}^{\dagger}_{-q'}(t)]e^{i(q+q')la}, \tag{34}$$

$G^{2}(q)$ is still given by Eq. (10b), and

$$f(q,q')=\frac{N_{L}\pi e^{2}}{mcV\sqrt{|qq'|}}. \tag{35}$$

We remind that two-level atom is only a working hypothesis, it does not meet the basic condition that the total levels of atom form a complete set, so sometimes one needs to do some additional handling.[14] In $f(q,q')$, originally there is a factor $\mathbf{e}_\lambda\cdot\mathbf{e}_{\lambda'}$ and summation over λ and λ', where $\mathbf{e}_\lambda$ denotes polarization vectors of the photon with $\lambda=1,2$. For an atom with a complete set of eigenstates $|n\rangle$, we have

$$\begin{aligned}\mathbf{e}_\lambda\cdot\mathbf{e}_{\lambda'}&=\langle 1|\mathbf{e}_\lambda\cdot\mathbf{e}_{\lambda'}|1\rangle\\&=\frac{-i}{\hbar}\sum_n[\langle 1|\mathbf{e}_\lambda\cdot\mathbf{x}|n\rangle\langle n|\mathbf{e}_{\lambda'}\cdot\mathbf{p}|1\rangle-\langle 1|\mathbf{e}_{\lambda'}\cdot\mathbf{p}|n\rangle\\&\quad\times\langle n|\mathbf{e}_\lambda\cdot\mathbf{x}|1\rangle]\\&=\frac{m}{\hbar}\sum_n\Omega_{n1}[\langle 1|\mathbf{e}_\lambda\cdot\mathbf{x}|n\rangle\langle n|\mathbf{e}_{\lambda'}\cdot\mathbf{x}|1\rangle+\langle 1|\mathbf{e}_{\lambda'}\cdot\mathbf{x}|n\rangle\\&\quad\times\langle n|\mathbf{e}_\lambda\cdot\mathbf{x}|1\rangle]\\&=\frac{m}{\hbar e^2}\sum_n\Omega_{n1}[(\mathbf{e}_\lambda\cdot\mathbf{d}_{1n})(\mathbf{e}_{\lambda'}\cdot\mathbf{d}_{n1})+(\mathbf{e}_{\lambda'}\cdot\mathbf{d}_{1n})\\&\quad\times(\mathbf{e}_\lambda\cdot\mathbf{d}_{n1})].\end{aligned}\tag{36}$$

In the two-level approximation, Eq. (36) reduces to

$$\mathbf{e}_\lambda\cdot\mathbf{e}_{\lambda'}\cong\frac{2m\Omega}{\hbar e^2}(\mathbf{e}_\lambda\cdot\mathbf{d})(\mathbf{e}_{\lambda'}\cdot\mathbf{d}),\tag{37}$$

where Ω stands for Ω_{21} and $\mathbf{d}=\mathbf{d}_{21}=\mathbf{d}_{12}$. Taking $\mathbf{e}_\lambda$ such that

$$\mathbf{e}_1\cdot\mathbf{d}=d,\quad \mathbf{e}_2\cdot\mathbf{d}=0,$$

Eq. (37) reduces to

$$\mathbf{e}_\lambda\,.\mathbf{e}_{\lambda'}\cong\frac{2m\Omega d^2}{\hbar e^2}\delta_{\lambda 1}\delta_{\lambda'\lambda}\,.\tag{38}$$

Adding $\Sigma_{\lambda,\lambda'}\mathbf{e}_\lambda\cdot\mathbf{e}_{\lambda'}$ in Eq. (35) and utilizing Eq. (38), we get

$$f(q,q')=\frac{2\pi N_L\Omega d^2}{c\hbar V\sqrt{|qq'|}}=\frac{1}{N\Omega}G(q)G(q').\tag{39}$$

This is the desired modification. We note in passing that the physical implication of Eq. (38) is

$$m\Omega|x_{12}|^2=x_{12}|p_{12}|=\frac{\hbar}{2}.$$

Substituting Eq. (39) into Eq. (34) and making use of

$$\sum_l e^{i(q+q')la}=N\sum_k O(q'-k)O(k+q),\tag{40}$$

we get the amended $\hat{H}_{int}(t)$ as

$$\begin{aligned}\hat{H}_{int}(t)&=\hbar\sum_{q,k}G(q)O(k+q)[\hat{B}_k(t)+\hat{B}^\dagger_{-k}(t)]\\&\quad\times[\hat{a}_q(t)+\hat{a}_{-q}(t)]+\hbar\sum_{q,q'k}\frac{1}{\Omega}G(q)G(q')\\&\quad\times O(q'-k)O(k+q)[\hat{a}_q(t)+\hat{a}^\dagger_{-q}(t)]\\&\quad\times[\hat{a}_{q'}(t)+\hat{a}^\dagger_{-q'}(t)].\end{aligned}\tag{41}$$

The equations for $\hat{B}_k(t)$ and $\hat{B}^\dagger_{-k}(t)$ remain unaltered, while the equations for $\hat{a}_q(t)$ and $\hat{a}^\dagger_{-q}(t)$ have an additional term:

$$\begin{aligned}i\frac{\partial}{\partial t}\hat{a}_q(t)&=|q|c\hat{a}_q(t)+G(q)\sum_k O(k-q)[\hat{B}_k(t)+\hat{B}^\dagger_{-k}(t)]\\&\quad+\frac{2}{\Omega}\sum_{q',k}G(q)G(q')O(q'-k)O(k-q)\\&\quad\times[\hat{a}_{q'}(t)+\hat{a}^\dagger_{-q'}(t)],\end{aligned}\tag{42a}$$

$$\begin{aligned}i\frac{\partial}{\partial t}\hat{a}^\dagger_{-q}(t)&=-|q|c\hat{a}^\dagger_{-q}(t)-G(q)\sum_k O(k-q)\\&\quad\times[\hat{B}_k(t)+\hat{B}^\dagger_{-k}(t)]\\&\quad-\frac{2}{\Omega}\sum_{q',k}G(q)G(q')O(q'-k)O(k-q)\\&\quad\times[\hat{a}_{q'}(t)+\hat{a}^\dagger_{-q'}(t)].\end{aligned}\tag{42b}$$

Performing the half side Fourier transformation of Eqs. (42) as before, and eliminate $\Sigma_{q'}G(q')O(q'-k)\times[\hat{a}_{q'}(\omega)+\hat{a}^\dagger_{-q'}(\omega)]$ therein by use of Eqs. (13c) and (13d), we get

$$\begin{aligned}(\omega-|q|c)\hat{a}_q(\omega)&=G(q)\sum_k\frac{1}{\Omega}O(k-q)\{\omega[\hat{B}_k(\omega)\\&\quad-\hat{B}^\dagger_{-k}(\omega)]-i[\hat{B}_k(0)-\hat{B}^\dagger_{-k}(0)]\}\\&\quad+i\hat{a}_q(0),\end{aligned}\tag{43a}$$

$$\begin{aligned}(\omega+|q|c)\hat{a}^\dagger_{-q}(\omega)&=-G(q)\sum_k\frac{1}{\Omega}O(k-q)\{\omega[\hat{B}_k(\omega)\\&\quad-\hat{B}^\dagger_{-k}]-i[\hat{B}_k(0)-\hat{B}^\dagger_{-k}(0)]\}\\&\quad+i\hat{a}^\dagger_{-q}(0)\end{aligned}\tag{43b}$$

to replace Eqs. (13a) and (13b). Equations (13c) and (13d) together with Eqs. (43a) and (43b) form our revised simultaneous equations. Eliminating $\hat{a}_q(\omega)$ and $\hat{a}^\dagger_{-q}$ from these equations, we get, instead of Eq. (22), a revised dynamical equation for exciton operator:

$$\begin{aligned}&\sum_{k'}\left[(\omega^2-\Omega^2)\delta_{kk'}-\frac{2\omega^2}{\Omega}F_{kk'}(\omega)\right][\hat{B}_{k'}(\omega)-\hat{B}^\dagger_{-k'}(\omega)]\\&=-2i\frac{\omega}{\Omega}\sum_{k'}F_{kk'}(\omega)[\hat{B}_{k'}(0)-\hat{B}^\dagger_{-k'}(0)]\\&\quad+i[(\omega+\Omega)\hat{B}_k(0)-(\omega-\Omega)\hat{B}^\dagger_{-k}(0)]\\&\quad+2i\omega\sum_q G(q)O(k-q)\left[\frac{1}{\omega-|q|c}\hat{a}_q(0)\right.\\&\quad\left.+\frac{1}{\omega+|q|c}\hat{a}^\dagger_{-q}(0)\right],\end{aligned}\tag{44}$$

where $F_{kk'}(\omega)$ is the same as that in Sec. II. Comparing Eq. (44) with Eq. (22), we see that in the left-hand side $F_{kk'}(\omega)$

is replaced by $(\omega^2/\Omega^2)F_{kk'}(\omega)$ and $\hat{B}_{k'}(\omega)+\hat{B}^\dagger_{-k'}(\omega)$ is changed to $\hat{B}_{k'}(\omega)-\hat{B}^\dagger_{-k'}(\omega)$. The right-hand side is also altered. These modifications will lead to reasonable values for decay rate and frequency shift, as we see in the next sections.

Solving Eq. (44) for $\hat{B}_k(\omega)-\hat{B}^\dagger_{-k}(\omega)$ and substituting it into Eqs. (43a) and (43b) to get

$$\hat{a}_q(\omega)-\hat{a}^\dagger_{-q}(\omega)=\frac{2\omega}{\Omega^2(\omega^2-q^2c^2)}G(q)\sum_k O(k-q)\times\{\omega[\hat{B}_k(\omega)-\hat{B}^\dagger_{-k}(\omega)]-i[\hat{B}_k(0)-\hat{B}^\dagger_{-k}(0)]\}+\frac{i}{\omega-|q|c}\hat{a}_q(0)-\frac{i}{\omega+|q|c}\hat{a}^\dagger_{-q}(0), \tag{45}$$

the time evolution of electromagnetic (e.m.) field operators may be derived still by Eqs. (23) and (24). We note that both the stimulated emission and reabsorption effects have already been taken into account.

V. SINGLE LATTICE-LAYER CASE: ELECTRIC FIELD, LIGHT INTENSITY, COHERENCE, AND STATISTICS PROPERTIES

In this section, the case of monolayer $(N=1)$ will be studied in detail. The characteristic equation for decay rates and frequency shifts now becomes

$$\omega^2-\Omega^2-\frac{2\omega^2}{\Omega}F_{00}(\omega)=0. \tag{46a}$$

Substituting Eq. (25) in it yields

$$\omega^2+i\eta\omega-\Omega^2=0 \tag{46b}$$

which just have two physical roots given by

$$\omega_{1,2}=-\frac{1}{2}i\eta\pm\Omega_0,\quad \Omega_0=\sqrt{\Omega^2-\frac{1}{4}\eta^2}\cong\Omega\left(1-\frac{\eta^2}{8\Omega^2}\right). \tag{46c}$$

Thus the problems which arises in the coupling $(e/mc)\mathbf{P}\cdot\mathbf{A}$ and coupling $-\mathbf{E}\cdot\mathbf{d}$ are eliminated.

The term $(e^2/2mc^2)\mathbf{A}^2$ is usually regarded as unimportant in treating the emission process, however, in our problem we see it is not so. We also see that in our problem the two interactions $(e/mc)\mathbf{P}\cdot\mathbf{A}+(e^2/2mc^2)\mathbf{A}^2$ and $-\mathbf{E}\cdot\mathbf{d}$ are not equivalent to each other. As pointed out by many authors,[15] in the full quantum theory although one can use an unitary transformation to transform the $(e/mc)\mathbf{P}\cdot\mathbf{A}+(e^22mc^2)\mathbf{A}^2$ interaction to $-\mathbf{d}\cdot\hat{\mathbf{E}}$ interaction plus a term $\int\mathbf{P}_\perp^2 d\tau$, but in the new basis, the operator $\hat{\mathbf{E}}$ actually has the meaning of electric displacement, not the electric field, and satisfies a different dynamical equation. It is easy to see that if a factor ω^2/q^2c^2 is added in the integrand of $F_{kk'}(\omega)$ for $-\mathbf{d}\cdot\hat{\mathbf{E}}$ interaction, the corresponding characteristic equation will become the same as that for $(e/mc)\mathbf{P}\cdot\hat{\mathbf{A}}+(e^2/2mc^2)\hat{\mathbf{A}}^2$. We note that the factor ω^2/q^2c^2 also expresses the difference between the right-hand sides of Eqs. (2.12) and (2.14) in the first paper of Ref. 15.

To see the photon field generated by exciton fluorescence, we drop the terms proportional to $\hat{a}_q(0)$ or $\hat{a}^\dagger_{-q}(0)$ in Eqs. (44) and (45), and hence get

$$\hat{B}_0(\omega)-\hat{B}^\dagger_0(\omega)=i\frac{(\omega+\Omega+i\eta)\hat{B}_0(0)-(\omega-\Omega+i\eta)\hat{B}^\dagger_0(0)}{\omega^2+i\eta\omega-\Omega^2}. \tag{47}$$

It gives in turn that

$$\hat{a}_q(\omega)-\hat{a}^\dagger_{-q}(\omega)=\frac{2i\omega G(q)}{\omega^2-q^2c^2}\,\frac{(\omega+\Omega)\hat{B}_0(0)+(\omega-\Omega)\hat{B}^\dagger_0(0)}{\omega^2+i\eta\omega-\Omega^2}. \tag{48}$$

In the region $z>0$ outside the layer, the integral in Eq. (24) can be evaluated by adding an infinite half circle in the upper complex q plane. Substituting Eq. (48) into it yields

$$\hat{E}(z,\omega)=i\sqrt{\frac{\pi\hbar\Omega\eta}{cA}}\frac{(\omega+\Omega)\hat{B}_0(0)+(\omega-\Omega)\hat{B}^\dagger_0(0)}{\omega^2+i\eta\omega-\Omega^2}e^{i(\omega/c)z}. \tag{49}$$

We remind that A is the area of the layer, it is also the cross area of the normalization volume for the photon.

The electric field $\hat{E}(z,t)$ in the $z>0$ region generated by the exciton is then calculated by Eq. (23). For the case $z-ct>0(<0)$, one may add an infinite upper (lower) half circle in the ω plane to form a closed contour. The results so obtained are given by

$$\hat{E}(z,t)=0,\quad \text{for}\quad z-ct>0, \tag{50a}$$

$$\hat{E}(z,t)=\hat{\mathcal{E}}^{(+)}(z,t)+\text{H.c.}\quad \text{for}\quad z-ct<0 \tag{50b}$$

in which

$$\hat{\mathcal{E}}^{(+)}(z,t)=\sqrt{\frac{\pi\hbar\Omega\eta}{4cA}}\left[\left(1+\frac{\Omega}{\Omega_0}-\frac{i}{2}\frac{\eta}{\Omega_0}\right)\hat{B}_0(0)+\left(1-\frac{\Omega}{\Omega_0}-\frac{i}{2}\frac{\eta}{\Omega_0}\right)\hat{B}^\dagger_0(0)\right]\times e^{-i\Omega_0(t-z/c)-(1/2)\eta(t-z/c)}, \tag{51}$$

and $\Omega_0-\Omega$ stands for the frequency shift.

Equation (50a) is the consequence of the result that all the roots of the characteristic equation are in the lower half plane of complex variable ω. The previous characteristic equation [Eq. (29)] has a root in the upper half ω plane, hence it violates the requirement that emitted field should be zero in spacelike interval.

Equations (50b) and (51) show the exciton-generated electric field in $z>0$ region behaves like a damped wave propagating in forward direction as required. No peak develops. The decay is of exponential type, demonstrating the cooperation of radiation is from beginning to the end.

For reference, we write down the neglected part in $\hat{E}(z,t)$, which is proportional to $\hat{a}_q(0)$ and $\hat{a}_q^\dagger(0)$, as $\hat{E}'(z,t)+\hat{E}^{(0)}(z,t)$:

$$\hat{E}'(z,t)=\sum_q \sqrt{\frac{\pi\hbar\eta^2}{2V|q|c}}\Bigg[\left(\frac{\left(\Omega_0-\frac{i}{2}\eta\right)^2 e^{-i\Omega_0(t-z/c)-(1/2)\eta(t-z/c)}}{\Omega_0\left(\Omega_0-|q|c-\frac{1}{2}i\eta\right)}-\frac{2|q|^2c^2e^{-i|q|c(t-z/c)}}{\left(\Omega_0-|q|c-\frac{i}{2}\eta\right)\left(\Omega_0+|q|c+\frac{i}{2}\eta\right)}\right)\hat{a}_q(0)+\frac{\left(\Omega_0-\frac{i}{2}\eta\right)^2 e^{-i\Omega_0(t-z/c)-(1/2)\eta(t-z/c)}}{\Omega_0\left(\Omega_0+|q|c-\frac{1}{2}i\eta\right)}\hat{a}_q^\dagger(0)\Bigg]+\text{H.c.} \tag{52a}$$

for $z-ct>0$, and $\hat{E}'(z,t)$ equals zero for $z-ct<0$, while

$$\hat{E}^{(0)}(z,t)=i\sum_q \sqrt{\frac{2\pi\hbar|q|c}{V}}\hat{a}_q(0)e^{iqz-i|q|ct}+\text{H.c.}, \tag{52b}$$

it is just the free varying photon field. We note that $\hat{E}'(z,t)$ is proportional to η namely proportional to the square of coupling constant.

$\hat{E}(z,t)$ in $z<0$ region can be derived similarly. The result is a damped wave propagating in the backward z direction instead. The polarization vector of electric field is along the transition dipole moment $\mathbf{d}$ which is assumed lying in the plane of slab.

The magnetic field can be derived from the electric field through Maxwell equations. One sees that the energy flux $\hat{\mathbf{S}}$ is directed outward from the crystal film, both in $z>0$ and in $z<0$ sides. We note that the above solution is free from Markov approximation and also free from rotating wave approximation.

The decay rate of emission intensity equals to η, which can be reexpressed by

$$\eta=3\left(\frac{\pi\lambda\!\!\!^{-2}}{a^2}\right)\gamma, \tag{53}$$

where γ is the Einstein A coefficient of an isolated lattice atom, $\lambda\!\!\!^{-}$ denotes the reduced wavelength, namely c/Ω. Outwardly, only a number of $3(\pi\lambda\!\!\!^{-2}/a^2)$ atoms, i.e., number of lattice sites in an area $3(\pi\lambda\!\!\!^{-2})$, are involved in cooperation. Nevertheless, it is not the true physics. From Eqs. (9) and (10) it is seen that for $N=1$, $G=\sqrt{N_L}g$, and $\hat{B}_k=(1/\sqrt{N_L})\Sigma_j\hat{b}_j$, hence all atoms in the layer are involved in cooperation, they interact with photon collectively. The factor $3(\pi\lambda\!\!\!^{-2}/a^2)$ actually comes from the reduction of available photon states in our one-dimension model as compared with that of isolated atom, which will be explained in the following.

In one-dimension model, the number of photon states within the range dk is $2(L/2\pi)dk$, the factor 2 counts the two sides of the slab, while in the three-dimension case the corresponding number of photon states is $(L/2\pi)^3 4\pi k^2 dk$. The reduction factor is then

$$\alpha=2\left(\frac{L}{2\pi}\right)\Big/\left(\frac{L}{2\pi}\right)^3 4\pi k^2=\frac{2\pi}{k^2L^2} \tag{54}$$

which equals $2(\pi\lambda\!\!\!^{-2}/L^2)$ at the frequency Ω. Thus the enhancement factor, α times the number of cooperation, turns out to be

$$\alpha N_T=\alpha\frac{L^2}{a^2}=2\left(\frac{\pi\lambda\!\!\!^{-2}}{a^2}\right). \tag{55}$$

There is still a factor $\frac{2}{3}$ of difference, which is due to our assumption that the dipole moment lies in the plane of the crystal film.

We now study the coherence and statistical properties as well as the evolution of intensity of the emitted e.m. field. From Eqs. (50b) and (51),

$$\langle\hat{E}(z,t)\rangle=\sqrt{\frac{\pi\hbar\Omega\eta}{4cA}}\Bigg[\left(1+\frac{\Omega}{\Omega_0}-\frac{i}{2}\frac{\eta}{\Omega_0}\right)\langle\hat{B}_0(0)\rangle+\left(1-\frac{\Omega}{\Omega_0}-\frac{i}{2}\frac{\eta}{\Omega_0}\right)\times\langle\hat{B}_0^\dagger(0)\rangle\Bigg]e^{-i\Omega_0(t-z/c)-(\eta/2)(t-z/c)}+\text{c.c.}, \tag{56}$$

hence if initially the exciton is in chaotic state, number state or in general a state with density matrix diagonal in Fock representation, $\langle\hat{E}(z,t)\rangle$ will be zero for all times, which means no coherent part will develop in the emitted (e.m.) field, even though the radiation is cooperative. When the exciton is initially in coherent state, a coherence part of emitted field results consequently. However, the emitted field is not exactly in a coherent state as we shall see below Eq. (59).

It seems that the ''$\hat{E}^{(+)}(z,t)$ part'' of $\hat{E}(z,t)$ for $z-ct<0$ is just $\hat{\mathcal{E}}^{(+)}(z,t)$ defined by Eq. (51), since it is a damped wave with positive frequency. However, this is not true according to the original definition. The original definition of $\hat{E}^{(+)}(z,t)$ is the part consisting of photon annihilation operators:

$$\begin{aligned}\hat{E}^{(+)}(z,t)&=\frac{i}{2\pi}\int_{-\infty}^{+\infty}dq\int_{-\infty+i\epsilon}^{+\infty+i\epsilon}d\omega\sqrt{\frac{|q|c\hbar L}{2\pi A}}\hat{a}_q(\omega)\\&\quad\times e^{i(qz-\omega t)}\\&=\frac{-1}{2\pi}\int_{-\infty}^{+\infty}dq\int_{-\infty+i\epsilon}^{+\infty+i\epsilon}d\omega\\&\quad\times\sqrt{\frac{\Omega\hbar c\eta}{4\pi A}}\frac{1}{\omega-|q|c}\\&\quad\times\frac{(\omega+\Omega)\hat{B}_0(0)+(\omega-\Omega)\hat{B}_0^\dagger(0)}{\omega^2+i\eta\omega-\Omega^2}e^{i(qz-\omega t)}.\end{aligned}\tag{57}$$

The integration respect to q cannot be carried out analytically because of the factor $1/(\omega-|q|c)$. We can only arrive at the following results:

$$\hat{E}^{(+)}(z,t)=0\tag{58a}$$

for $t<0$, and

$$\hat{E}^{(+)}(z,t)=\sqrt{\frac{\pi\Omega\hbar\eta}{4Ac}}[F_1(z,t)\hat{B}_0(0)+F_2(z,t)\hat{B}_0^\dagger(0)]\tag{58b}$$

for $t>0$, in which

$$\begin{aligned}F_1(z,t)=\frac{i}{\pi}\int_0^{\omega_M}d\omega_q\Bigg[&\frac{2(\omega_q+\Omega)e^{-i\omega_q t}}{\left(\omega_q-\Omega_0+\frac{i}{2}\eta\right)\left(\omega_q+\Omega_0+\frac{i}{2}\eta\right)}\\&-\frac{\left(\Omega_0+\Omega-\frac{i}{2}\eta\right)e^{-i\Omega_0 t-(1/2)\eta t}}{\Omega_0\left(\omega_q-\Omega_0+\frac{i}{2}\eta\right)}\\&-\frac{\left(\Omega_0-\Omega+\frac{i}{2}\eta\right)e^{i\Omega_0 t-(1/2)\eta t}}{\Omega_0\left(\omega_q+\Omega_0+\frac{i}{2}\eta\right)}\Bigg]\cos\left(\omega_q\frac{z}{c}\right),\end{aligned}\tag{58c}$$

$$\begin{aligned}F_2(z,t)=\frac{i}{\pi}\int_0^{\omega_M}d\omega_q\Bigg[&\frac{2(\omega_q-\Omega)e^{-i\omega_q t}}{\left(\omega_q-\Omega_0+\frac{i}{2}\eta\right)\left(\omega_q+\Omega_0+\frac{i}{2}\eta\right)}\\&-\frac{\left(\Omega_0-\Omega-\frac{i}{2}\eta\right)e^{-i\Omega_0 t-(1/2)\eta t}}{\Omega_0\left(\omega_q-\Omega_0+\frac{i}{2}\eta\right)}\\&-\frac{\left(\Omega_0+\Omega+\frac{i}{2}\eta\right)e^{i\Omega_0 t-(1/2)\eta t}}{\Omega_0\left(\omega_q+\Omega_0+\frac{i}{2}\eta\right)}\Bigg]\cos\left(\omega_q\frac{z}{c}\right),\end{aligned}\tag{58d}$$

where $\omega_q\equiv|q|c$, ω_M is the cutoff frequency due to our dipole approximation with the value $\omega_M\sim c/a$. Actually one may write the upper limit of integration as ∞, since it is convergent when $\omega_M\to\infty$, and c/a is already sufficiently large. All the integrals in Eqs. (58) can be expressed by complex Si and Ci functions. We see that the third terms in the square brackets are components of negative frequency.

The operator $\hat{a}_q(t)$ may also be calculated by Eqs. (43a) and (47) with the result

$$\begin{aligned}\hat{a}_q(t)=G(q)\Bigg[&\frac{(\omega_q+\Omega)\hat{B}_0(0)+(\omega_q-\Omega)\hat{B}_0^\dagger(0)}{\left(\omega_q-\Omega_0+\frac{i}{2}\eta\right)\left(\omega_q+\Omega_0+\frac{i}{2}\eta\right)}e^{-i\omega_q t}-\frac{\left(\Omega_0+\Omega-\frac{i}{2}\eta\right)\hat{B}_0(0)+\left(\Omega_0-\Omega-\frac{i}{2}\eta\right)\hat{B}_0^\dagger(0)}{2\Omega_0\left(\omega_q-\Omega_0+\frac{i}{2}\eta\right)}\\&\times e^{-i\Omega_0 t-(\eta/2)t}-\frac{\left(\Omega_0-\Omega+\frac{i}{2}\eta\right)\hat{B}_0(0)+\left(\Omega_0+\Omega+\frac{i}{2}\eta\right)\hat{B}_0^\dagger(0)}{2\Omega_0\left(\Omega_0+\omega_q+\frac{i}{2}\eta\right)}e^{i\Omega_0 t-(\eta/2)t}\Bigg].\end{aligned}\tag{59}$$

This equation shows that the eigenstate of $\hat{B}_0(0)$ is not just the eigenstate of $\hat{a}_q(t)$ because of the terms proportional to $\hat{B}_0^\dagger(0)$, confirming that the emitted field is not exactly in a coherent state as mentioned below Eq. (56).

Since electromagnetic interaction is weak, we shall not take account of dressing effect. For example, the Heisenberg state in which initially there is one physical exciton is just taken as $\hat{B}_0^\dagger(0)|0\rangle$, where $|0\rangle$ is the bare vacuum state. The light intensity of a state $|\rangle$ is now defined as

$$I(z,t)=\frac{c}{2\pi}\langle|:\hat{E}^{(-)}(z,t)\hat{E}^{(+)}(z,t):|\rangle=\frac{c}{2\pi}[\langle|\hat{E}^{(-)}(z,t)\hat{E}^{(+)}(z,t)|\rangle-\langle 0|\hat{E}^{(-)}(z,t)\hat{E}^{(+)}(z,t)|0\rangle]. \tag{60}$$

where the symbol :: means the normal product according to $\hat{B}_0(0)$ and $\hat{B}_0^\dagger(0)$. Similarly, the first-order degree of coherence of emitted field is given by

$$g^{(1)}(z,t;z,t+\tau)=\frac{\langle|\hat{E}^{(-)}(z,t)\hat{E}^{(+)}(z,t+\tau)|\rangle-\langle 0|\hat{E}^{(-)}(z,t)\hat{E}^{(+)}(z,t+\tau)|0\rangle}{\frac{2\pi}{c}\sqrt{I(z,t)I(z,t+\tau)}}. \tag{61}$$

When the exciton initially is in a state with density matrix diagonal in Fock representation (including chaotic state and number state), we have

$$g^{(1)}(z,t;z,t+\tau)=\frac{F_1^*(z,t)F_1(z,t+\tau)+F_2^*(z,t)F_2(z,t+\tau)}{[F_1^*(z,t)F_1(z,t)+F_2^*(z,t)F_2(z,t)]^{1/2}[F_1^*(z,t+\tau)F_1(z,t+\tau)+F_2^*(z,t+\tau)F_2(z,t+\tau)]^{1/2}}. \tag{62}$$

For initial exciton in coherent state $|\alpha\rangle$, $g^{(1)}(z,t;z,t+\tau)$ may be obtained by following formulas:

$$\begin{aligned}&\langle\alpha|\hat{E}^{(-)}(z,t)\hat{E}^{(+)}(z,t+\tau)|\alpha\rangle\\&\quad-\langle 0|\hat{E}^{(-)}(z,t)\hat{E}^{(+)}(z,t+\tau)|0\rangle\\&=\frac{\Omega\hbar\eta}{4\pi Ac}[|\alpha|^2F_1^*(z,t)F_1(z,t+\tau)\\&\quad+|\alpha|^2F_2^*(z,t)F_2(z,t+\tau)+\alpha^2F_2^*(z,t)F_1(z,t+\tau)\\&\quad+\alpha^{*2}F_1^*(z,t)F_2(z,t+\tau)]\end{aligned} \tag{63}$$

and similar expression for $I(z,t)$ and $I(z,t+\tau)$ in its denominator, where α is the eigenvalue of $\hat{B}_0(0)$, namely $\hat{B}_0(0)|\alpha\rangle=\alpha|\alpha\rangle$.

We note that in case the antirotating terms in $\hat{E}^{(+)}(z,t)$, which include the term proportional to $F_2(z,t)$ as well as the negative frequency term in $F_1(z,t)$, are dropped, the $g^{(1)}(z,t;z,t+\tau)$ will be independent of the initial condition of the excitons. However, numerical calculation shows that $F_2(z,t)$ is not negligible as compared with $F_1(z,t)$. As to the negative frequency term in $F_1(z,t)$, it is indeed negligibly small. Numerical calculation also shows that $\hat{E}^{(+)}(z,t)$ is quite different from $\hat{\mathcal{E}}^{(+)}(z,t)$. The magnitude of the coefficient of $\hat{B}_0(0)$ in $\hat{E}^{(+)}$ is less than that in $\hat{\mathcal{E}}^{(+)}(z,t)$ while the magnitude of the coefficient of $\hat{B}_0^+(0)$ in $\hat{E}^{(+)}$ is much larger than that in $\hat{\mathcal{E}}^{(+)}(z,t)$.

A striking result is that the $I(z,t)$ defined by Eq. (60) oscillates rapidly with frequency Ω_0 and soon afterwards quivers irregularly with time, contrary to what people usually expect. In Fig. 1 some numerical curves are given to show this time evolution. For comparison we also plot the curve for $\mathcal{I}(z,t)$ defined by $\hat{\mathcal{E}}^{(+)}$ as

$$\mathcal{I}(z,t)=\frac{c}{2\pi}\langle|:\hat{\mathcal{E}}^{(-)}(z,t)\hat{\mathcal{E}}^{(+)}(z,t):|\rangle. \tag{64}$$

The values of $\mathcal{I}(z,t)$ are obtained by substituting $[1+\Omega/\Omega_0-(i/2)\eta/\Omega_0]e^{-i\Omega_0(t-z/c)-(1/2)\eta(t-z/c)}$ for $F_1(z,t)$ and substituting $[1-\Omega/\Omega_0-(i/2)\eta/\Omega_0]e^{-i\Omega_0(t-z/c)-(1/2)\eta(t-z/c)}$ for $F_2(z,t)$ in Eqs. (62) and (63). We see from Fig. 1 that $\mathcal{I}(z,t)$ is slightly below the smoothed $I(z,t)$.

$\mathcal{I}(z,t)$ also has its own meaning. It is just the cycle average of the expectation value of energy flux operator $\hat{S}(z,t)=(c/4\pi):\hat{E}(z,t)^2:$. The role of cycle average is to eliminate the rapid oscillating terms $(c/4\pi)\langle|:\hat{\mathcal{E}}^{(-)}(z,t)^2:|\rangle$ and $(c/4\pi)\langle|:\hat{\mathcal{E}}^{(+)}(z,t)^2:|\rangle$.

Another striking result is that $I(z,t)$ does not vanish immediately as $|z|$ goes beyond $ct(t>0)$ to enter the spacelike region but gradually drops down as shown in Fig. 2. This result may be regarded as an exhibition that $\hat{E}^{(+)}(z,t)$ does not have the meaning of annihilating a photon at position z. As a contrast, $\hat{E}(z,t)$ does vanish immediately as $|z|$ goes beyond ct [see Eq. (50a)] which is a natural result from the retarded solution.

The absolute values of $g^{(1)}$ are shown in Fig. 3, together with the absolute values of $\mathcal{G}^{(1)}$, in which the $\hat{\mathcal{E}}^{(\pm)}$ are used to substitute $\hat{E}^{(\pm)}$. The curves for $|\mathcal{G}^{(1)}|$ are all straight lines with height always equal to 1, no matter the initial exciton state is coherent or with density matrix diagonal in Fock representation. The curves for $|g^{(1)}|$ are different. In the case that the density matrix of the initial exciton state is diagonal in Fock representation, $|g^{(1)}|$ first oscillates rapidly and soon afterwards quivers irregularly around a nearly straight line with height $|g^{(1)}|=0.8$. A striking result is that for coherent initial exciton state the $|g^{(1)}|$ keeps equal to 1 without any vibration. It is also independent of θ, the phase of α.

The second degree of coherence $g^{(2)}(z,t;z,t+\tau)$ is now defined by

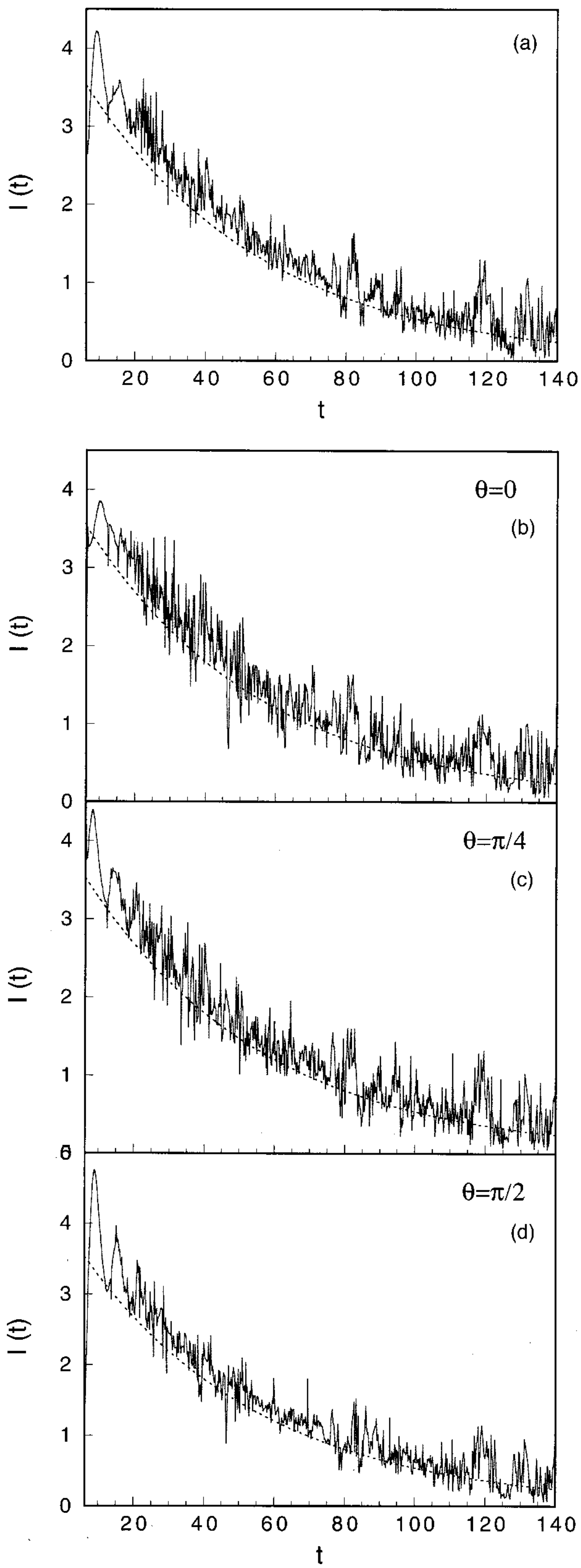

FIG. 1. Time evolution of light intensities $I(z,t)$ at point $z=2\pi c/\Omega$. I is in units of $\frac{1}{8}\langle n\rangle\hbar\Omega(\eta/A)$, where $\langle n\rangle$ is the initial mean number of excitons. t is in units of $1/\Omega$. $\eta/2\Omega=10^{-2}$. The dashed lines represent $\mathcal{I}(z,t)$. (a) The case that the density matrix of initial exciton state is diagonal in Fock representation, including the chaotic state and number state. (b)–(d) The cases that the initial exciton state is coherent state with eigenvalue $\alpha=|\alpha|e^{i\theta}$.

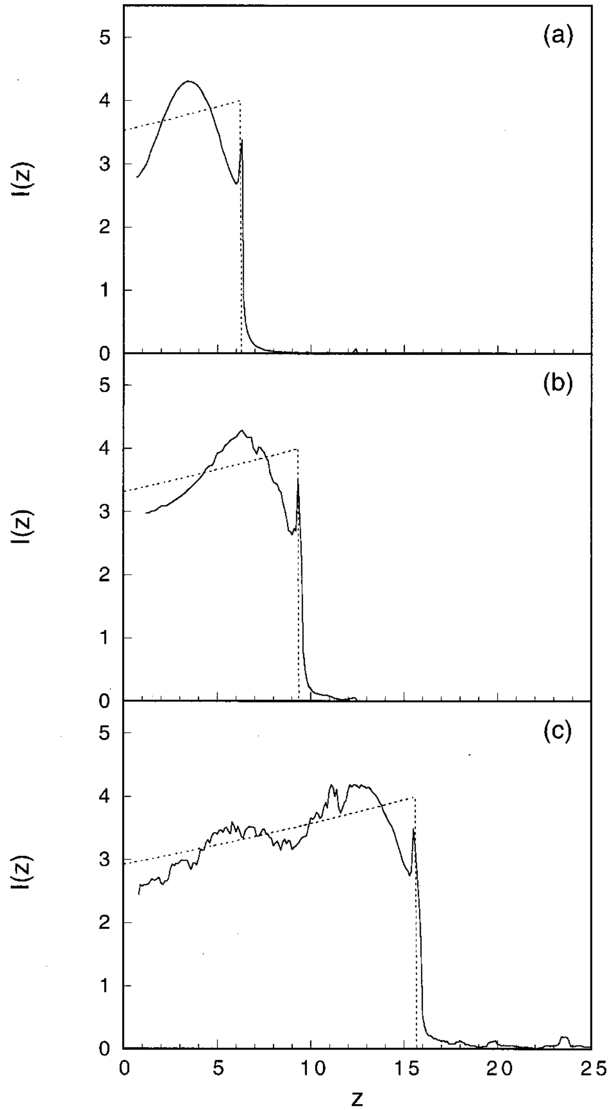

FIG. 2. Space distribution of intensity $I(z,t)$. (a) $t=2\pi/\Omega$, (b) $t=3\pi/\omega$, (c) $t=5\pi/\omega$. I is in units of $\frac{1}{8}\langle n\rangle\hbar\Omega\,\eta/A$, $z-ct$ is in units of c/Ω, $\eta/\Omega=10^{-2}$. The dashed line represents $\mathcal{I}(z,t)$. The initial exciton is in chaotic state or number state.

$$g^{(2)}(z,t;z,t+\tau)$$
$$=\frac{\langle|\hat{E}^{(-)}(z,t)\hat{E}^{(-)}(z,t+\tau)\hat{E}^{(+)}(z,t+\tau)\hat{E}^{(+)}(z,t)|\rangle}{\frac{4\pi^2}{c^2}I(z,t)I(z,t+\tau)}$$
$$-\frac{\langle 0|\hat{E}^{(-)}(z,t)\hat{E}^{(-)}(z,t+\tau)\hat{E}^{(+)}(z,t+\tau)\hat{E}^{(+)}(z,t)|0\rangle}{\frac{4\pi^2}{c^2}I(z,t)I(z,t+\tau)}. \tag{65}$$

For comparison we also plot the curves of $|\mathcal{G}^{(2)}(z,t;z,t+\tau)|$ by substituting $\hat{\mathcal{E}}^{(\pm)}$ for $\hat{E}^{(\pm)}$ in Eq. (65).

The results for chaotic initial exciton states are shown in Fig. 4. We see that $|\mathcal{G}^{(2)}|$ is always equal to 2 and does not

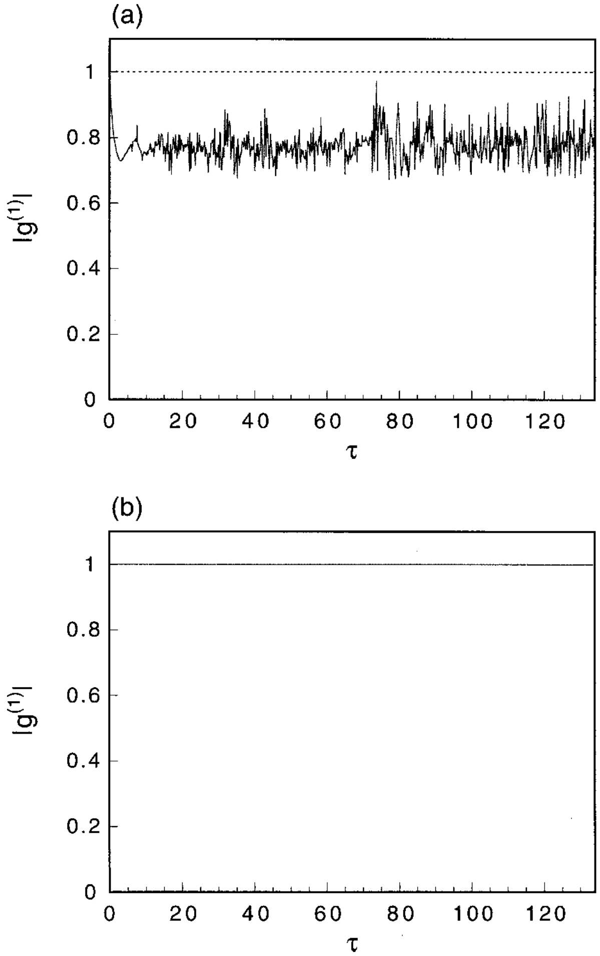

FIG. 3. The absolute value of first-order degree of coherence $g^{(1)}(z,t;z,t+\tau)$ as a function of $\tau. z=2\pi$, $t=2\pi$. t and τ are in units of $1/\Omega$ and z is in units of c/Ω. $\eta/2\Omega=10^{-2}$. (a) The case that the density matrix of initial exciton state is diagonal in Fock representation. The dashed line represents $|\mathcal{G}^{(1)}(z,t;z,t+\tau)|$. (b) The case that the initial exciton state is coherent. $|\mathcal{G}^{(1)}(z,t;z,t+\tau)|$ coincides with $|g^{(1)}(z,t;z,t+\tau)|$.

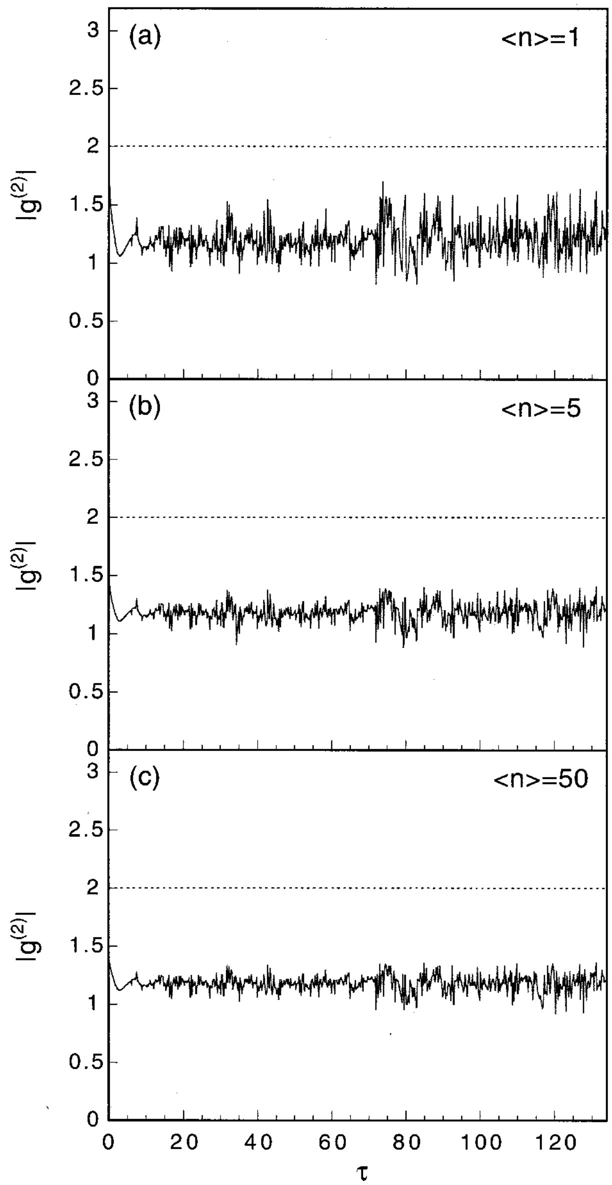

FIG. 4. The absolute value of second-order degree of coherence $g^{(2)}(z,t;z,t+\tau)$ as a function of τ for chaotic initial exciton states. $z=2\pi$, $t=2\pi$. t and τ are in units of $1/\Omega$ and z is in units of c/Ω. $\eta/2\Omega=10^{-2}$. The dashed lines represent $|\mathcal{G}^{(2)}(z,t;z,t+\tau)|$. (a) The mean initial exciton number $n=1$. (b) The case $n=5$. (c) The case $n=50$.

drop down when time difference becomes large, while $|g^{(2)}|$ fluctuates around about 1.2 and shows only small differences for different values of $\langle n\rangle$. These results mean that despite superradiance, the light generated by such excitons is bunching, but not serious. For initial number exciton states, $|\mathcal{G}^{(2)}|$ is almost given by $1-1/n$ as can be seen from Fig. 5, while $|g^{(2)}|$ shows less dependence on n. When $n=50$, it still vibrates around 0.6, hence quite evident antibunching remains.

The $|g^{(2)}|$ and $|\mathcal{G}^{(2)}|$ for coherent initial states are shown in Fig. 6. All curves for $|\mathcal{G}^{(2)}|$ are equal to 1, independent of $\langle n\rangle$ and θ where $\langle n\rangle^{(1/2)}e^{i\theta}=\alpha$. However, the situation for $|g^{(2)}|$ is quite different. For small $\langle n\rangle$ such as $\langle n\rangle=1$, $|g^{(2)}|$ is relatively high, vibrating around the horizontal line 2.1 for $\theta=0$ and $\theta=\pi/4$, and around the horizontal line 3.3 for $\theta=\pi/2$. When $\langle n\rangle$ becomes larger, such as 5, $|g^{(2)}|$'s mean values decrease to the range 1.2–1.5, depending on the value θ. For still larger value of $\langle n\rangle$, say 50, the mean values of $|g^{(2)}|$ further decrease to 1.04 for $\theta=0$ and $\pi/4$, and about 1.22 for $\theta=\pi/2$. Another notable feature is when θ keeps fixed and $\langle n\rangle$ becomes larger, the amplitude of fluctuation becomes smaller, while for fixed $\langle n\rangle$ the fluctuation is larger in the case of $\theta=\pi/2$ than those of $\theta=0$ and $\theta=\pi/4$.

The above results indicate explicitly that despite the investigated exciton superfluorescence is totally collective, its coherence and statistics still have diverse possibilities.

VI. CASE OF DOUBLE AND TRIPLE LATTICE LAYERS

We have studied the single lattice layer case in some detail. In this section we will turn to study the fluorescence of Frenkel exciton in double and triple lattice layers. For small values of N, it is more convenient to use the sum $\Sigma_l e^{i(k+q)la}$ instead of $[\sin\frac{1}{2}N(k+q)a]/[\sin\frac{1}{2}(k+q)a]$ for $O(k+q)$ in the integrand of Eq. (18) and then evaluate the integral by contour integration directly. All eigendecay rates, frequency shifts as well as the time evolution of fields are obtained consequently.

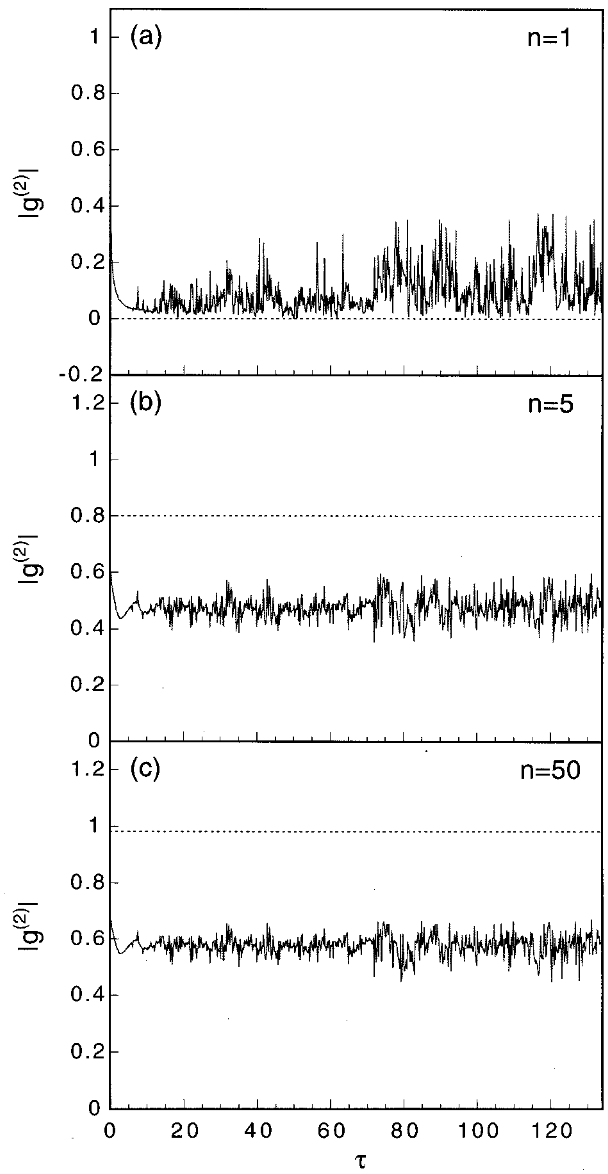

FIG. 5. The absolute value of second-order degree of coherence $g^{(2)}(z,t;z,t+\tau)$ as a function of τ for excitons initially in number states. $z=2\pi$, $t=2\pi$. t and τ are in units of $1/\Omega$, z is in units of c/Ω. $\eta/2\Omega=10^{-2}$. The dashed lines represent $|\mathcal{G}^{(2)}(z,t;z,t+\tau)|$. (a) The case $n=1$. n is the initial exciton number. (b) The case $n=5$. (c) The case $n=50$.

First, we consider the special case $N=2$. The values of m in Eq. (8) now take $-1/2$ and $1/2$ corresponding to $k=\pm\pi/2a$, respectively We shall use $F_{++}(\omega),F_{--}(\omega)$ to represent $F_{+\pi/2a,+\pi/2a}(\omega),F_{-\pi/2a,-\pi/2a}(\omega)$, etc. and evaluate the integrals in Eq. (18) by substituting $\frac{1}{2}[e^{-i(1/2)(k-q)a}+e^{i(1/2)(k-q)a}]$ for $O(k-q)$. The results are given by

$$F_{++}(\omega)=F_{--}(\omega)=-i\frac{\eta\Omega}{\omega},$$

$$F_{+-}(\omega)=F_{-+}(\omega)=-i\frac{\eta\Omega}{\omega}e^{i\omega a/c}. \tag{66}$$

One sees that the nondiagonal elements (F_{+-} and F_{-+}) is of the same order as the diagonal elements (F_{++} and F_{--}).

The coupled Eq. (44) now becomes

$$(\omega^2+i\omega\eta-\Omega^2)[\hat{B}_+(\omega)-\hat{B}_-^\dagger(\omega)] +i\omega\eta e^{i\omega a/c}[\hat{B}_-(\omega)-\hat{B}_+^\dagger(\omega)]=\hat{A}_0(w), \tag{67a}$$

$$i\omega\eta e^{i\omega a/c}[\hat{B}_+(\omega)-\hat{B}_-^\dagger(\omega)]+(\omega^2+i\omega\eta-\Omega^2) \times[\hat{B}_-(\omega)-\hat{B}_+^\dagger(\omega)]=-\hat{A}_0^\dagger(-\omega), \tag{67b}$$

where

$$\hat{A}_0(\omega)=i[(\omega+\Omega+i\eta)\hat{B}_+(0)-(\omega-\Omega+i\eta)\hat{B}_-^\dagger(0)] -\eta e^{i\omega a/c}[\hat{B}_-(0)-\hat{B}_+^\dagger(0)] +2\sqrt{2}\omega i\sum_q G(q)\cos\left(\frac{\pi}{4}-\frac{qa}{2}\right) \times\left(\frac{\hat{a}_q(0)}{\omega-|q|c}+\frac{\hat{a}_{-q}^\dagger(0)}{\omega+|q|c}\right), \tag{67c}$$

$$\hat{A}_0^\dagger(-\omega)=i[(\omega-\Omega+i\eta)\hat{B}_+^\dagger(0)-(\omega+\Omega+i\eta)\hat{B}_-(0)] -\eta e^{i\omega a/c}[\hat{B}_-^\dagger(0)-\hat{B}_+(0)] -2\sqrt{2}\omega i\sum_q G(q)\cos\left(\frac{\pi}{4}+\frac{qa}{2}\right) \times\left(\frac{\hat{a}_q(0)}{\omega-|q|c}+\frac{\hat{a}_{-q}^\dagger(0)}{\omega+|q|c}\right). \tag{67d}$$

Equations (67) are easily solved to get

$$\hat{B}_+(\omega)-\hat{B}_-^\dagger(\omega)=\frac{(\omega^2+i\omega\eta-\Omega^2)\hat{A}_0(\omega)+i\omega\eta e^{i\omega a/c}\hat{A}_0^\dagger(-\omega)}{(\omega^2+i\omega\eta-\Omega^2+i\omega\eta e^{i\omega a/c})(\omega^2+i\omega\eta-\Omega^2-i\omega\eta e^{i\omega a/c})}, \tag{68a}$$

$$\hat{B}_-(\omega)-\hat{B}_+^\dagger(\omega)=-\frac{i\omega\eta e^{i\omega a/c}\hat{A}_0(\omega)+(\omega^2+i\omega\eta-\Omega^2)\hat{A}_0^\dagger(-\omega)}{(\omega^2+i\omega\eta-\Omega^2+i\omega\eta e^{i\omega a/c})(\omega^2+i\omega\eta-\Omega^2-i\omega\eta e^{i\omega a/c})}. \tag{68b}$$

The roots of characteristic equations

$$\omega^2+i\omega\eta-\Omega^2+i\omega\eta e^{i\omega a/c}=0 \tag{69a}$$

and

$$\omega^2+i\omega\eta-\Omega^2-i\omega\eta e^{i\omega a/c}=0 \tag{69b}$$

will determine the eigendecay rates and corresponding frequency shifts. All roots of Eqs. (69) will have negative imaginary part, since two necessary conditions can be deduced for this equation to have root of positive imaginary part:

$$\eta>2\Omega \quad \text{and} \quad \frac{\eta a}{c}>2\pi,$$

and both of these conditions are untenable. Similarly, Eq. (69b) cannot have root of positive imaginary part either. These results mean the basic physics laws will not be violated as in the case of monolayer.

Assuming the physical roots ω_j of Eqs. (69) are not far away from $\pm\Omega$ (hence $|\omega_j|a/c\ll 1$), we expand the factor $e^{i\omega a/c}$ up to second order of $\omega a/c$. By this way four physical roots of Eqs. (69) are obtained as follows:

$$\omega_1=\Omega_1-i\Gamma_1,\quad \omega_3=-\Omega_1-i\Gamma_1,$$
$$\omega_2=\Omega_2-i\Gamma_2,\quad \omega_4=-\Omega_2-i\Gamma_2 \tag{70}$$

in which

$$\Omega_1\cong\Omega\left(1-\frac{\eta^2}{2\Omega^2}+\frac{\eta a}{2c}\right),\quad \Gamma_1\cong\eta,$$

$$\Omega_2\cong\Omega\left(1-\frac{\eta a}{2c}\right),\quad \Gamma_2\cong\frac{1}{4}\eta\frac{\Omega^2a^2}{c^2}. \tag{71}$$

In the following we will omit the terms proportional to $\hat{a}_q(0),\hat{a}_q^\dagger(0)$, since here we just study the fluorescence of excitons. Substituting Eq. (68) and

$$\hat{a}_q(\omega)-\hat{a}^\dagger_{-q}(\omega)=\frac{2\omega\sqrt{N}}{\Omega(\omega^2-q^2c^2)}G(q)\sum_k O(k-q)$$
$$\times\{\omega[\hat{B}_k(\omega)-\hat{B}^\dagger_{-k}(\omega)]$$
$$-i[\hat{B}_k(0)-\hat{B}^\dagger_{-k}(0)]\} \tag{72}$$

into Eq. (24) and carrying out the contour integration, we get $\hat{E}(z,\omega)$ in the positive z region outside the crystal slab as

$$\hat{E}(z,\omega)=i\frac{2\pi\Omega d}{ac\sqrt{A}}\left(\cos\frac{\omega a}{2c}\,\frac{(\omega+\Omega)[\hat{B}_+(0)+\hat{B}_-(0)]+(\omega-\Omega)[\hat{B}^\dagger_+(0)+\hat{B}^\dagger_-(0)]}{\omega^2+i\omega\eta-\Omega^2+i\omega\eta e^{i\omega a/c}}\right.$$
$$\left.+\sin\frac{\omega a}{2c}\,\frac{(\omega+\Omega)[\hat{B}_+(0)-\hat{B}_-(0)]-(\omega-\Omega)[\hat{B}^\dagger_+(0)-\hat{B}^\dagger_-(0)]}{\omega^2+i\omega\eta-\Omega^2-i\omega\eta e^{i\omega a/c}}\right)e^{(i\omega/c)z}, \tag{73}$$

where A is the area of each layer, it is also the cross area of the normalization volume for the photon as mentioned above.

The electric field $\hat{E}(z,t)$ in this region is calculated by Eq. (23), with the results given by

$$\hat{E}(z,t)=0,\ \text{for } z-ct>0, \tag{74a}$$

$$\hat{E}(z,t)=\hat{\mathcal{E}}^{(+)}(z,t)(z,t)+\text{H.c.},\quad \text{for } z-ct<0, \tag{74b}$$

where

$$\hat{\mathcal{E}}^{(+)}(z,t)=\frac{f}{c}\sqrt{\frac{\pi\hbar\Omega a}{8A}}\left(1+\frac{\Omega}{\Omega_1}-i\frac{\Gamma_1}{\Omega_1}\right)\cos\frac{(\Omega_1-i\Gamma_1)a}{2c}\left\{[\hat{B}_+(0)+\hat{B}_-(0)]+\frac{\Omega_1-\Omega-i\Gamma_1}{\Omega_1+\Omega-i\Gamma_1}\right.$$
$$\left.\times[\hat{B}^\dagger_+(0)+\hat{B}^\dagger_-(0)]\right\}e^{-i\Omega_1(t-z/c)-\Gamma_1(t-z/c)}+\frac{f}{c}\sqrt{\frac{\pi\hbar\Omega a}{8A}}\left(1+\frac{\Omega}{\Omega_2}-i\frac{\Gamma_2}{\Omega_2}\right)\sin\frac{(\Omega_2-i\Gamma_2)a}{2c}$$
$$\times\left\{[\hat{B}_+(0)-\hat{B}_-(0)]-\frac{\Omega_2-\Omega-i\Gamma_2}{\Omega_2+\Omega-i\Gamma_2}[\hat{B}^\dagger_+(0)-\hat{B}^\dagger_-(0)]\right\}e^{-i\Omega_2(t-z/c)-\Gamma_2(t-z/c)}. \tag{75}$$

Like the case $N=1$, we see that these are small components of $\hat{B}^\dagger_+(0)\pm\hat{B}^\dagger_-(0)$ mixed with $\hat{B}_+(0)\pm\hat{B}_-(0)$ in the $\hat{\mathcal{E}}^{(+)}(z,t)$, which is caused by antirotating interaction.

The electric field in the $z<0$ region can be derived similarly, with the resultant waves propagating in backward z direction as expected.

There are two eigendecay rates appeared in the $\hat{E}(z,t)$: Γ_1 and Γ_2. The corresponding eigenmodes are linear combi-

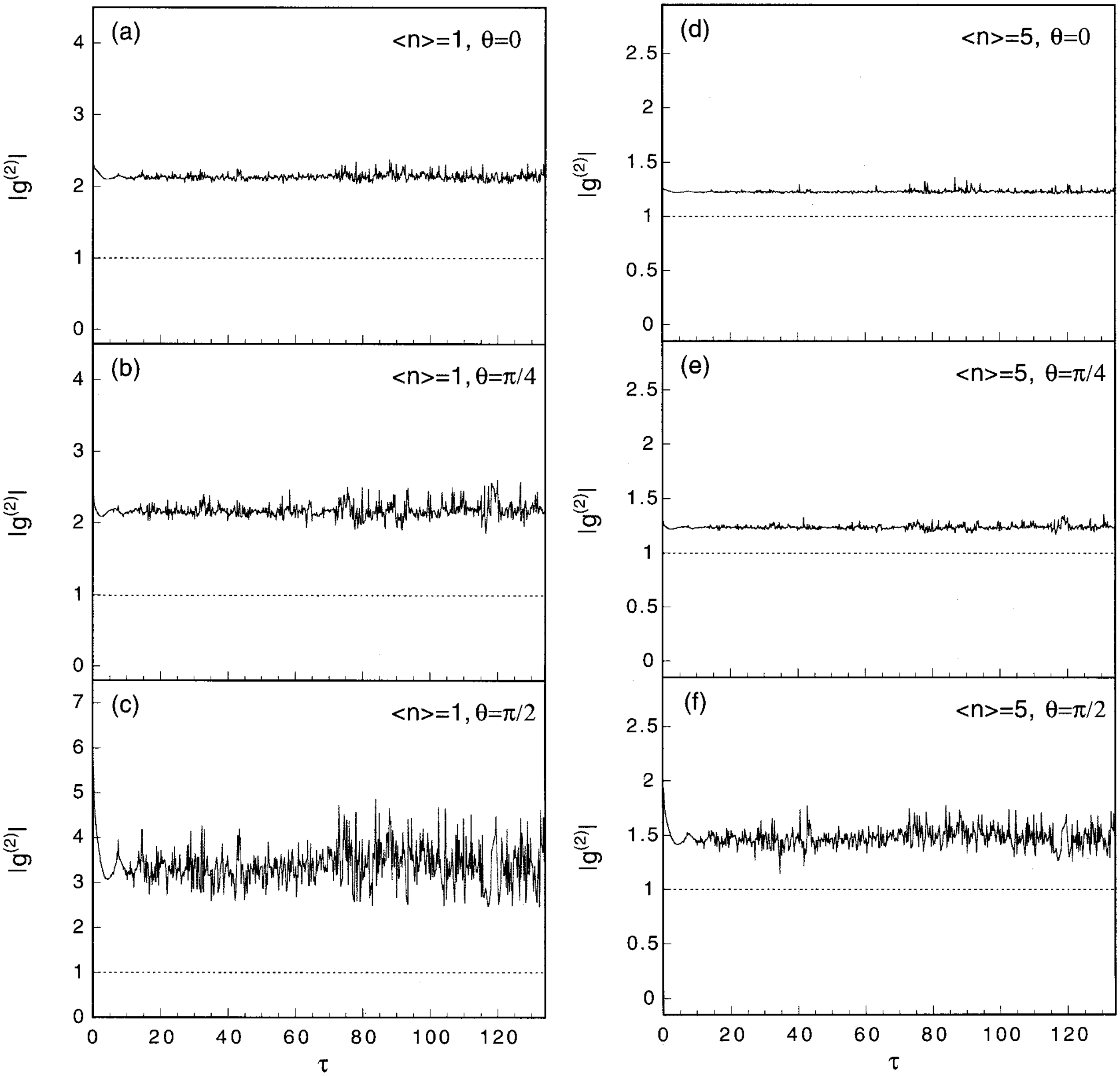

FIG. 6. The absolute value of second-order degree of coherence $g^{(2)}(z,t;z,t+\tau)$ as a function of τ for excitons initially in coherent state with eigenvalue $\alpha=|\alpha|e^{i\theta}$. $z=2\pi$, $t=2\pi$. t and τ are in units of $1/\Omega$, z is in units of c/Ω. $\eta/2\Omega=10^{-2}$. The dashed lines represent $|\mathcal{G}^{(2)}(z,t;z,t+\tau)|$. (a) The case $\langle n\rangle=|\alpha|^2=1,\theta=0$. (b) The case $\langle n\rangle=|\alpha|^2=1,\theta=\pi/4$. (c) The case $\langle n\rangle=|\alpha|^2=1,\theta=\pi/2$. (d) The case $\langle n\rangle=|\alpha|^2=5,\theta=0$. (e) The case $\langle n\rangle=|\alpha|^2=5,\theta=\pi/4$. (f) The case $\langle n\rangle=|\alpha|^2=5,\theta=\pi/2$. (g) The case $\langle n\rangle=|\alpha|^2=50,\theta=0$. (h) The case $\langle n\rangle=|\alpha|^2=50,\theta=\pi/4$. (i) The case $\langle n\rangle=|\alpha|^2=50,\theta=\pi/2$.

nation of the two modes of $m=\frac{1}{2}$ and $m=-\frac{1}{2}$. As can be-seen from Eq. (75), these two eigenmodes correspond to the operators $(1/\sqrt{2})[\hat{B}_+(0)+\hat{B}_-(0)]$ and $(1/\sqrt{2})[\hat{B}_+(0)-\hat{B}_-(0)]$, respectively. Hence they correspond to modes of $m=0$ $(k=0)$ and $m=1$ $(k=\pi/a)$ with the operators

$$\hat{B}_0(t)=\frac{1}{\sqrt{2}}[\hat{B}_{l=-1/2}(t)+\hat{B}_{l=1/2}(t)]=\frac{1}{\sqrt{2}}[\hat{B}_+(t)+\hat{B}_-(t)], \tag{76}$$

$$\hat{B}_1(t)=\frac{i}{\sqrt{2}}[\hat{B}_{l=-1/2}(t)-\hat{B}_{l=1/2}(t)]=\frac{1}{\sqrt{2}}[\hat{B}_+(t)-\hat{B}_-(t)]. \tag{77}$$

We see from Eq. (71) that $m=0$ mode is the superradiant mode and $m=1$ mode is the subradiant mode. The dipoles of the two layers have the same phase for the former and have opposite phase for the latter. By Eq. (53), the decay rate Γ_2 of subradiant mode is still as large as $3\pi/4$ times γ, the decay rate of a single atom (molecular), because the atoms in each layer are still cooperated. The decay rate of $k=0$ mode is nearly twice that of monolayer, which is just the character of superfluorescence. The above result also shows: when values of k are taken as symmetrical set $k=\pm\pi/2a$, which are required by our mathematical formation, the coupling between two exciton modes is most important. But for unsymmetrical set $k=0$ and $k=1$ there is no coupling between two corresponding modes.

As discussed in last section, even for the superradiant

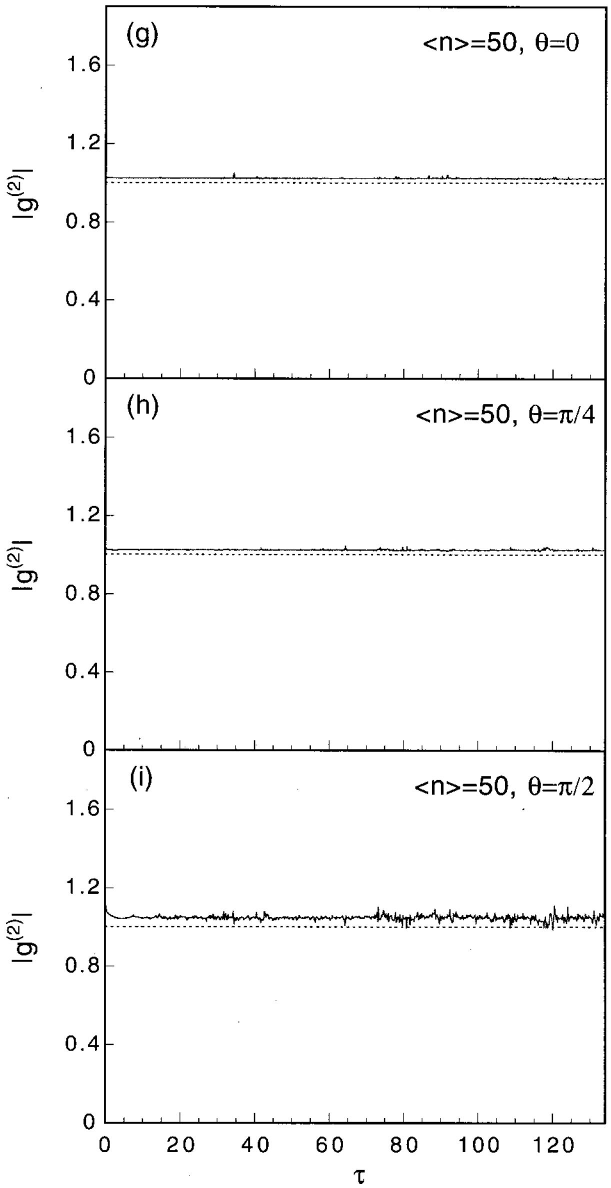

FIG. 6. (*Continued*).

mode in which the emission is totally collective, the emitted light still may have different statistics and coherence properties according to the initial exciton state. For example, from Eq. (75) the coherent part of the electric field $\langle \hat{E}(z,t)\rangle$ will be nonzero when the initial state of the exciton is a coherent state, and when the initial density matrix of the exciton is diagonal in Fock representation (including number state, chaotic state), the coherent part of $\langle \hat{E}(z,t)\rangle$ will be zero.

Up to the first order of $\Omega a/c$ and η/Ω, the $\hat{E}(z,t)$ is expressed by the superradiant mode operator $\hat{B}_0(0)$ and the subradiant mode operator $\hat{B}_1(0)$ as follows:

$$\hat{E}(z,t)=\sqrt{\frac{2\pi\eta\hbar\Omega}{cA}}\left(\hat{B}_0(0)-\frac{i\eta}{2\Omega}\hat{B}_0^{\dagger}(0)\right)\times e^{-i\Omega_1(t-z/c)-\Gamma_1(t-z/c)}+\sqrt{\frac{2\pi\eta\hbar\Omega}{cA}}\left(\frac{\Omega a}{2c}\right)\times\hat{B}_1(0)e^{-i\Omega_2(t-z/c)-\Gamma_2(t-z/c)}+\text{H.c.} \tag{78}$$

for $z>0$ and $t-z/c>0$. Similar results may be obtained for $z<0,t+z/c>0$. $\hat{E}(z,t)$ is equal to zero if $(z>0,t-z/c<0)$ or $(z<0,t+z/c<0)$.

We already have seen irregular behaviors of the usual intensity operator in the single layer case, here only the energy flux operator is studied. The energy flux is defined by

$$\hat{\mathbf{S}}(z,t)=\frac{c}{4\pi}:\hat{\mathbf{E}}(z,t)\times\hat{\mathbf{B}}(z,t):. \tag{79}$$

It readily shows that $\hat{\mathbf{S}}$ is always directed outward from the crystal film. So we rewrite $\hat{\mathbf{S}}$ as $\mathbf{n}\hat{S}$, in which $\mathbf{n}$ is unit vector directing the outer space from lattice layers and $\langle \hat{S}(z,t)\rangle$ may be evaluated from Eq. (78). After neglecting oscillating terms and higher-order terms of η/Ω and $\Omega a/c$, we have

$$\begin{aligned}\langle \hat{S}(z,t)\rangle=&\frac{\eta\hbar\Omega}{A}\left(\langle \hat{B}_0^{\dagger}(0)\hat{B}_0(0)\rangle+\frac{i\eta}{2\Omega}\langle \hat{B}_0^{2}(0)\rangle\right.\\&\left.-\frac{i\eta}{2\Omega}\langle \hat{B}_0^{\dagger 2}(0)\rangle\right)e^{2\eta(z/c-t)}\\&+\frac{\eta'\hbar\Omega}{A}\langle \hat{B}_1^{\dagger}(0)\hat{B}_1(0)\rangle e^{2\eta'(z/c-t)}\\&+\frac{\sqrt{\eta\eta'}\hbar\Omega}{A}\left(\langle \hat{B}_0^{\dagger}(0)\hat{B}_1(0)\rangle+\langle \hat{B}_1^{\dagger}(0)\hat{B}_0(0)\rangle\right.\\&+\frac{i\eta}{2\Omega}\langle \hat{B}_1(0)\hat{B}_0(0)\rangle\\&\left.-\frac{i\eta}{2\Omega}\langle \hat{B}_1^{\dagger}(0)\hat{B}_0^{\dagger}(0)\rangle\right)e^{(\eta+\eta')(z/c-t)},\end{aligned} \tag{80a}$$

with

$$\eta'=\eta\frac{\Omega^2a^2}{4c^2}. \tag{80b}$$

We see from Eqs. (80) that the energy flux decays in three different rates. The first term, which is contributed by the exciton of the short lifetime, plays an important part at the beginning time. The second term contributed by the exciton of the long lifetime becomes dominant at the latter time of the process. The third term will exhibit itself in the intermediate stage.

Now we turn to the case of triple lattice layers. The cases of odd N and even N have a qualitative difference in the m-value series $-1/2(N-1),\ldots\frac{1}{2}(N-1)$. In the former case, m contains *zero*, while in the latter, it does not. $N=3$ is the simplest case of the former, apart from the trivial case $N=1$. Now $F_{m,m'}(\omega)$'s compose a 3×3 matrix $F(\omega)$ which will be written as

$$F(\omega)=-\frac{\eta\Omega}{6\omega}D(\omega). \tag{81}$$

In terms of $D_{m,m'}$, couple equations now take the form

$$(\omega^2-\Omega^2)[\hat{B}_m(\omega)-\hat{B}^\dagger_{-m}(\omega)]+\frac{1}{3}\eta\omega \times\sum_{m'} D_{mm'}(\omega)[\hat{B}_{m'}(\omega)-\hat{B}^\dagger_{-m'}(\omega)] = i[(\omega+\Omega)\hat{B}_m(0)-(\omega-\Omega)\hat{B}^\dagger_{-m}(0)] + \frac{i}{3}\eta\sum_{m'} D_{mm'}(\omega)[\hat{B}_{m'}(0)-\hat{B}^\dagger_{-m'}(0)] \quad (82a)$$

with

$$m,m'=-1,0,1. \quad (82b)$$

In Eqs. (82), terms proportional to $\hat{a}_q(0)$ and $\hat{a}^\dagger_{-q}(0)$ are neglected as we do below Eq. (71). From the simultaneous Eqs. (82), we get the characteristic equation as

$$(\omega^2-\Omega^2)^3+\tfrac{1}{3}\eta\omega(v+2u)(\omega^2-\Omega^2)^2+\tfrac{1}{9}\eta^2\omega^2 \times(2uv+u^2-s^2-2r^2)(\omega^2-\Omega^2) + \tfrac{1}{27}\eta^3\omega^3[(u^2-s^2)v+2r^2(s-u)]=0, \quad (83)$$

where u, v, r, and s are matrix elements of $D(\omega)$, defined by

$$D(\omega)=\begin{pmatrix} u(\omega) & r(\omega) & s(\omega)\\ r(\omega) & v(\omega) & r(\omega)\\ s(\omega) & r(\omega) & u(\omega)\end{pmatrix}. \quad (84)$$

For the mathematical detail, see Appendix B. Equation (83) can be solved approximately to get the eigendecay rates and frequency shifts, six roots are obtained as follows:

$$\omega_1=\Omega_1-i\Gamma_1,\quad \omega_1'=-\Omega_1-i\Gamma_1,$$
$$\omega_0=\Omega-i\Gamma,\quad \omega_0'=-\Omega_0-i\Gamma_0, \quad (85)$$
$$\omega_{-1}=\Omega_{-1}-i\Gamma_{-1},\quad \omega_{-1}'=-\Omega_{-1}-i\Gamma_{-1}$$

with

$$\Omega_1\cong\Omega\left(1-\frac{\eta a}{3c}\right),\quad \Gamma_1=\frac{1}{27}\eta\frac{\Omega^2a^2}{c^2}, \quad (86a)$$

$$\Omega_0\cong\Omega\left(1-\frac{9\eta_2}{8\Omega^2}+\frac{4\eta a}{3c}\right),\quad \Gamma_0=\frac{3}{2}\eta, \quad (86b)$$

$$\Omega_{-1}=\left(1-\frac{\eta a}{c}\right),\quad \Gamma_{-1}=\eta\frac{\Omega^2a^2}{c^2}. \quad (86c)$$

We see that all the roots are in the lower half plan of complex ω as they should be.

The direct way to solve for $\hat{B}_m(\omega)-\hat{B}^\dagger_{-m}(\omega)$ from Eq. (82) is to diagonalize the matrix $D(\omega)$. The required transformation matrix is denoted by $T(\omega)$ which satisfies the requirement

$$T(\omega)D(\omega)\tilde{T}(\omega)=\begin{pmatrix} D_1(\omega) & & \\ & D_0(\omega) & \\ & & D_{-1}(\omega)\end{pmatrix}. \quad (87)$$

In terms of $T_{m,m'}$ and $D_{m,m'}$ The result for $\hat{B}_m(\omega)-\hat{B}^\dagger_{-m}(\omega)$ is expressed by

$$\hat{B}_m(\omega)-\hat{B}^\dagger_{-m}(\omega)=\sum_{m'} T_{m',m}\frac{6i}{\omega^2-\Omega^2+\frac{1}{3}\eta\omega D_{m'}} \times[(\omega+\Omega+\tfrac{1}{3}\eta D_{m'})\hat{\beta}^{(1)}_{m'}(\omega,0) -(\omega-\Omega+\tfrac{1}{3}\eta D_{m'})\hat{\beta}^{(2)}_{m'}(\omega,0)] \quad (88a)$$

in which

$$\hat{\beta}^{(1)}_m(\omega,0)=\frac{1}{6}\sum_{m'} T_{mm'}(\omega)\hat{B}_{m'}(0),$$
$$\hat{\beta}^{(2)}_m(\omega,0)=\frac{1}{6}\sum_{m'} T_{mm'}(\omega)\hat{B}^\dagger_{-m'}(0). \quad (88b)$$

Substituting Eqs. (88) into Eqs. (72) to get the expression for $\hat{a}_q(\omega)-\hat{a}^\dagger_{-q}(\omega)$, then $\hat{E}(z,\omega)$ is obtained by carrying out the integration over q in Eq. (24). Finally we get the solution for $\hat{E}(z,t)$ by Eq. (23):

$$\hat{E}(z,t)=\sqrt{\frac{3\pi\eta\hbar\Omega}{cA}}\theta\left(t-\frac{z}{c}\right)\sum_m \hat{\alpha}_m e^{-i\Omega_m(t-z/c)-\Gamma_m(t-z/c)} +\text{H.c.} \quad (89a)$$

for $z>0, t-z/c>0$, where

$$\hat{\alpha}_m=\frac{1}{\Omega_m}\sum_{m'}\left[2\cos\left(\frac{2\pi m'}{3}-\frac{\omega_m a}{c}\right)+1\right]T_{mm'}(\omega_m) \times[(\Omega+\omega_m)\hat{\beta}^{(1)}_m(\omega_m,0)-(\Omega-\omega_m)\hat{\beta}^{(2)}_m(\omega_m,0)]. \quad (89b)$$

The mode corresponding to $\hat{\alpha}_0$ is superradiant, its decay rate is three times of that of monolayer. The other two corresponding to $\hat{\alpha}_\pm$ are subradiant modes. The $\hat{\alpha}_m$'s can be derived approximately (cf. Appendix B), to the leading term, they are given by

$$\hat{\alpha}_1\cong i\frac{\Omega a}{9c}[\hat{B}_1(0)+\hat{B}_{-1}(0)],$$
$$\hat{\alpha}_0\cong\hat{B}_0(0), \quad (90)$$
$$\hat{\alpha}_{-1}\cong\frac{\Omega a}{\sqrt{3}c}[\hat{B}_1(0)-\hat{B}_{-1}(0)].$$

We see that the two exciton modes corresponding $m=\pm1$ are not of eigendecay rates. On the contrary, the eigenmodes are nearly the maximum mixture of these two modes. This means for the two subradiant modes, the coupling between modes of different k is important. As to the superradiant mode, only small components of $m=\pm 1$ modes are mixed to the $k=0$ mode [cf. Eq. (B5) of Appendix B].

In terms of the operators for annihilation on excitation in the lth layer $\hat{B}_l$, the annihilation operator for the three eigenmodes are approximately expressed by

$$\frac{1}{\sqrt{2}}[\hat{B}_{m=1}(0)+\hat{B}_{m=-1}(0)]$$

$$=\frac{1}{\sqrt{6}}[-\hat{B}_{l=1}(0)+2\hat{B}_{l=0}(0)-\hat{B}^{\dagger}_{l=-1}], \tag{91a}$$

$$\hat{B}_{m=0}=\frac{1}{\sqrt{3}}[\hat{B}_{l=1}(0)+\hat{B}_{l=0}(0)+\hat{B}_{l=-1}(0)], \tag{91b}$$

$$\frac{1}{\sqrt{2}}[\hat{B}_{m=1}(0)-\hat{B}_{m=-1}(0)]=\frac{i}{\sqrt{2}}[\hat{B}_{l=1}(0)-\hat{B}_{l=-1}(0)]. \tag{91c}$$

We see that in the superradiant mode$(m=0)$ the three $\hat{B}_l$'s are added constructively, hence the emission is totally cooperative. However, as in the previous cases, the statistical properties of the light of this mode still may have different varieties, depending on the initial state of the excitons. As to the two subradiant modes, the operators of three layers are superposed destructively, resulting in a long time emission.

For the $z>a$ region, the energy flux is given by

$$\langle\hat{S}(z,t)\rangle=\langle\hat{S}_1(z,t)\rangle+\langle\hat{S}_2(z,t)\rangle, \tag{92}$$

where $\langle\hat{S}_1(z,t)\rangle$ is the main part, it is expressed by

$$\langle\hat{S}_1(z,t)\rangle=\frac{\hbar\Omega\eta}{6A}\Bigg\{9\langle\hat{B}^{\dagger}_0(0)\hat{B}_0(0)\rangle e^{-3\eta(t-z/c)}$$

$$+\frac{2\Omega^2a^2}{9c^2}\langle\hat{B}^{\dagger}_+(0)\hat{B}_+(0)\rangle e^{-(8\eta'/27)(t-z/c)}$$

$$+\frac{6\Omega^2a^2}{c^2}\langle(\hat{B}^{\dagger}_-(0)\hat{B}_-(0)\rangle e^{-8\eta'(t-z/c)}\Bigg\} \tag{93a}$$

with $\hat{B}_\pm(0)=(1/\sqrt{2})[\hat{B}_1(0)\pm\hat{B}_{-1}(0)]$ and $\langle\hat{S}_2(z,t)\rangle$ is approximated by

$$\langle\hat{S}_2(z,t)\rangle=-i\frac{\hbar\Omega}{3\sqrt{3}A}\sqrt{\eta\eta'}[\langle\hat{B}^{\dagger}_+(0)\hat{B}_0(0)-\hat{B}^{\dagger}_0(0)\hat{B}_+(0)\rangle$$

$$+i3\sqrt{3}\langle\hat{B}^{\dagger}_-(0)\hat{B}_0(0)$$

$$-\hat{B}^{\dagger}_0(0)\hat{B}_-(0)\rangle]e^{-(3/2)\eta(t-Z/c)}. \tag{93b}$$

$\langle\hat{S}_2(z,t)\rangle$ only appears when the initial exciton density matrix in Fock representation has nondiagonal elements.

VII. BRIEF SUMMARY

In this paper we investigate the fluorescence of low density Frenkel excitons in a plane crystal slab. The excitons are assumed to be ideal bosons. The coupled Heisenberg equations of exciton operator and photon operators for arbitrary number of lattice layers are studied without Markov approximation and rotating wave approximation. The simplest case of single layer is first studied. When the interaction Hamiltonian is of type $(e/mc)\mathbf{P}\cdot\mathbf{A}$, the characteristic equation for the decay rate and frequency shift will have an unphysical root with negative decay rate. Change to the interaction of $-\mathbf{E}\cdot\mathbf{d}$ type, another unphysical result appears: the eigenfrequency drops down to zero. Only when the two-photon coupling term $(e^2/2mc^2)A^2$ is complemented to $(e/mc)\mathbf{P}\cdot\mathbf{A}$, the characteristic equation becomes reasonable. No unphysical root appears.

The superfluorescence of excitons in the case of single lattice layer is studied in detail. Some different features are shown as compared with the superfluorescence of atom aggregate:

(i) Actually, all the lattice atoms in the layer are involved in the cooperative radiation. That the decay rate η does not go infinite with increasing of number of lattice atoms is due to the reduction of the available photon states.

(ii) The cooperation of radiation exists almost from the beginning to the end, except at the very beginning.

(iii) The fluorescence intensity shows irregular quivers. These fluctuations are thought generated by the antirotating terms. We know that in the simple case where atom interacts with a single-mode light field, the antirotating term already induce additional rapid oscillations,[16] it is imaginable that in the case where atoms interact with multimode light field, these rapid oscillations of different frequencies will turn to irregular quivers.

(iv) The $\langle\hat{E}(z,t)\rangle$ is identical to zero outside the light cone $(|z|-ct>0)$, but the intensity $I(z,t)$ is not so. It penetrates outside the light cone to a small distance. This situation reminds us of the similar behavior of the photon propagator $\langle 0|T\hat{A}(\mathbf{x},t)\hat{A}(0,0)|0\rangle$ in the interaction picture, which is also not identical to zero in the spacelike region $r-ct>0$ (for $t>0$). This result shows that an atom may detect a photon in the region where $\langle\hat{E}\rangle$ is zero.

(v) Despite the fluorescence is of cooperative nature, the coherent and statistical properties of the emitted light still have various possibilities depending on the exciton initial conditions. The degrees of coherence $g^{(1)}$ and $g^{(2)}$ also show irregular fluctuations.

The cases of double and triple lattice layers are studied subsequently also by the interaction $(e/mc)\mathbf{P}\cdot\mathbf{A}+(e^2/2mc^2)\mathbf{A}^2$. Similarly no unphysical root of the characteristic equation is found. When the value of k is taken as the symmetrical set given by Eqs. (8), in general the coupling between the modes of different k cannot be neglected. In the double lattice-layer case, both the superradiant mode and subradiant mode are mixture of $k=\pm\pi/2a$ modes with equal weights. In the triple lattice layer case, the two subradiant modes are basically mixtures of $k=\pm\pi/a$ modes with equal weights, but the superradiant mode is mainly the $k=0$ mode.

ACKNOWLEDGMENTS

This research is a part of a project supported by National Natural Science Foundation of China (Grant No. 19774004) and is also supported by the International Program of National Science Foundation of USA (ECS-9800068). One of the authors (C. Q. Cao) thanks Professor F. Haake in Essen University for helpful discussions during his visit in Germany.

APPENDIX A: DERIVATION OF $F_{kk'}(\omega)$

To derive Eq. (20), we first substitute Eq. (10a) into Eq. (18), yielding

$$F_{kk'}(\omega)=-\frac{af^2\Omega}{4\pi c^2}\int_{-\infty}^{\infty}dq\,\frac{1}{N}\,\frac{\sin\frac{1}{2}(k-q)Na}{\sin\frac{1}{2}(k-q)a}\,\frac{\sin\frac{1}{2}(q-k')Na}{\sin\frac{1}{2}(q-k')a}\,\frac{1}{q^2-\frac{\omega^2}{c^2}}. \tag{A1}$$

As mentioned above, ω has an infinitesimal positive imaginary part; this determines how the integration path gets around the poles. It is easy to see that $F_{kk'}(\omega)=F_{k'k}(\omega)$ and $F_{kk'}(\omega)=F_{-k,-k'}(\omega)$. Expressing $\sin\frac{1}{2}(q-k')Na$ as difference of two exponentials, the corresponding two parts of integrand in Eq. (A1) vanish on the infinite half circles in the lower half q plane and upper half q plane, respectively. Note that $(a/2)(k-q)=n\pi$ are not poles of the original unseparated integrand, so we may take the integration path below these points or above these points by arbitrary choice. Contour integration gives the integral in Eq. (A1) as

$$\frac{\pi c}{2N\omega}\left[\frac{\sin\frac{1}{2}\left(k'+\frac{\omega}{c}\right)Na}{\sin\frac{1}{2}\left(k'+\frac{\omega}{c}\right)a}\,\frac{e^{(i/2)(k+\omega/c)Na}}{\sin\frac{1}{2}\left(k+\frac{\omega}{c}\right)a}-\frac{\sin\frac{1}{2}\left(k'-\frac{\omega}{c}\right)Na}{\sin\frac{1}{2}\left(k'-\frac{\omega}{c}\right)a}\,\frac{e^{-(i/2)(k-\omega/c)Na}}{\sin\frac{1}{2}\left(k-\frac{\omega}{c}\right)a}\right]$$
$$-\frac{2\pi}{Na}\,\frac{\sin\frac{1}{2}(k-k')Na}{\sin\frac{1}{2}(k-k')a}\sum_{n=-\infty}^{\infty}\frac{1}{\frac{\omega^2}{c^2}-\left(k+\frac{2n\pi}{a}\right)^2}.$$

In order to evaluate $\Sigma_{-\infty}^{\infty}1/[\omega^2/c^2-(k+2n\pi/a)^2]$, we note that above result holds for arbitrary k,k' and positive N. Take $N=1$, the integral in Eq. (A1) can be easily calculated with the result $\pi ic/\omega$. Through comparison we get

$$\sum_{n=-\infty}^{\infty}\frac{1}{\frac{\omega^2}{c^2}-\left(k+\frac{2n\pi}{a}\right)^2}=-\frac{ca}{4\omega}\,\frac{\sin\frac{\omega}{c}a}{\left[\sin\frac{1}{2}\left(k+\frac{\omega}{c}\right)a\right]\left[\sin\frac{1}{2}\left(k-\frac{\omega}{c}\right)a\right]}. \tag{A2}$$

In the extend $(\omega/c)a\ll 1$ and $ka\ll 1$, the right-hand side of Eq. (A2) may be approximated by $1/[(\omega^2/c^2-k^2)+\frac{1}{12}a^2]$, the second term stands for the small correction by the umklapp process, namely all the $n\neq 0$ terms in the summation. Substituting the above results into Eq. (A1), yields a closed expression of $F_{kk'}(\omega)$ for arbitrary N, which is just Eq. (20).

APPENDIX B: DERIVATION OF EIGENMODES AND DECAY RATES IN THE CASE OF TRIPLE LATTICE LAYERS

We substitute

$$O(k-q)=\tfrac{1}{3}[e^{-i(k-q)a}+1+e^{i(k-q)a}] \tag{B1}$$

into Eq. (18) and evaluate the integral term by term, we get the matrix composed by $F_{m,m'}(\omega)$ as

$$F(\omega)=-i\frac{\Omega\eta}{6\omega}\begin{pmatrix}-x^2-2x+3 & -x^2+x & 2x^2-2x\\ -x^2+x & 2x^2+4x+3 & -x^2+x\\ 2x^2-2x & -x^2+x & -x^2-2x+3\end{pmatrix}\equiv-\frac{\Omega\eta}{6\omega}D(\omega) \tag{B2}$$

with $x=e^{i\omega a/c}$. Writing the matrix elements of $D(\omega)$ as Eq. (84), the characteric equation is given by

$$\begin{vmatrix} \omega^2-\Omega^2+\frac{1}{3}\eta\omega u(\omega) & \frac{1}{3}\eta\omega r(\omega) & \frac{1}{3}\eta\omega s(\omega) \\ \frac{1}{3}\eta\omega r(\omega) & \omega^2-\Omega^2+\frac{1}{3}\eta\omega v(\omega) & \frac{1}{3}\eta\omega r(\omega) \\ \frac{1}{3}\eta\omega s(\omega) & \frac{1}{3}\eta\omega r(\omega) & \omega^2-\Omega^2+\frac{1}{3}\eta\omega u(\omega) \end{vmatrix}=0 \tag{B3}$$

which is just Eq. (83) in the text.

The roots ω_j of Eq. (83) are assumed not far from $\pm\Omega$, hence $|\omega_j|a/c \ll 1$. We may expand the factor $e^{i\omega a/c}$ into series. Up to second order of $(\omega a/c)^2$, the result is given by

$$u(\omega)=4\frac{\omega a}{c}+i3\left(\frac{\omega a}{c}\right)^2, \quad v(\omega)=9i-8\frac{\omega a}{c}-i6\left(\frac{\omega a}{c}\right)^2,$$

$$r(\omega)=\frac{\omega a}{c}+i\frac{3}{2}\left(\frac{\omega a}{c}\right)^2, \quad s(\omega)=-2\frac{\omega a}{c}-i3\left(\frac{\omega a}{c}\right)^2. \tag{B4}$$

We see that absolute values of u,r,s are small, only $|v|$ is large. Substituting Eq. (B4) into Eq. (83), one gets an algebraic equation of sixth order, its solution can be derived approximately. Results are those given by Eqs. (86).

The diagonalization of matrix D can be realized by two steps. First, use matrix

$$\begin{pmatrix} \frac{1}{\sqrt{2}} & 0 & \frac{1}{\sqrt{2}} \\ 0 & 1 & 0 \\ \frac{1}{\sqrt{2}} & 0 & -\frac{1}{\sqrt{2}} \end{pmatrix}$$

to transform D into

$$\begin{pmatrix} u(\omega)+s(\omega) & \sqrt{2}r(\omega) & 0 \\ \sqrt{2}r(\omega) & v(\omega) & 0 \\ 0 & 0 & u(\omega)-v(\omega) \end{pmatrix},$$

then find a 2×2 matrix to diagonalize

$$\begin{pmatrix} u(\omega)+s(\omega) & \sqrt{2}r(\omega) \\ \sqrt{2}r(\omega) & v(\omega) \end{pmatrix}.$$

By this way, we finally get

$$T(\omega)=\begin{pmatrix} \frac{1}{\sqrt{2}}M & -\frac{\sqrt{2}rM}{v-u-s} & \frac{1}{\sqrt{2}}M \\ \frac{rM}{v-u-s} & M & \frac{rM}{v-u-s} \\ \frac{1}{\sqrt{2}} & 0 & -\frac{1}{\sqrt{2}} \end{pmatrix}, \tag{B5a}$$

where

$$M(\omega)=\frac{1}{\sqrt{1+\frac{2r^2(\omega)}{[v(\omega)-u(\omega)-s(\omega)]^2}}}, \tag{B5b}$$

being of order 1. After solving Eq. (88), we get $\hat{a}_q(\omega)-\hat{a}^\dagger_{-q}(\omega)$ by Eq. (72),

$$\begin{aligned} \hat{a}_q(\omega)-\hat{a}^\dagger_{-q}(\omega)=&\frac{4\omega}{\omega^2-q^2c^2}G(q) \\ &\times\sum_{m,m'}\left[2\cos\left(\frac{2\pi m}{3}-qa\right)+1\right] \\ &\times\frac{iT_{m'm}}{\omega^2-\Omega^2+\frac{1}{3}\eta\omega D_{m'}} \\ &\times[(\Omega+\omega)\hat{\beta}^{(1)}_{m'}(\omega,0) \\ &-(\Omega-\omega)\hat{\beta}^{(2)}_{m'}(\omega,0)]. \end{aligned} \tag{B6}$$

Then carrying out the integral in Eq. (24) yields

$$\begin{aligned} \hat{E}(z,\omega)=&\frac{f}{c}\sqrt{\frac{6\pi\hbar\Omega}{A}}\sum_{m,m'} \\ &\times\left[2\cos\left(\frac{2\pi m}{3}-\frac{\omega a}{c}\right)+1\right]\frac{iT_{m'm}}{\omega^2-\Omega^2+\frac{1}{3}\eta\omega D_{m'}} \\ &\times[(\Omega+\omega)\hat{\beta}^{(1)}_{m'}(\omega,0)-(\Omega-\omega)\hat{\beta}^{(2)}_{m'}(\omega,0)] \end{aligned} \tag{B7}$$

which in turn leads to Eqs. (89).

*Mailing Address: Department of Physics, Peking University, Beijing 100871, China. Email address: cqcao@pku.edu.cn
†Email address: h-cao@northwestern.edu
‡Email address: liuyx@itp.ac.cn

[1] F.T. Arrechi and E. Courtens, Phys. Rev. A **2**, 1730 (1970).
[2] See, for example, C. Kittel, *Introduction to Solid State Physics*, sixth edition (John Wiley & Sons, New York, 1986), p. 300.
[3] E. Hanamura, Phys. Rev. B **38**, 1228 (1998).
[4] L.C. Andreani, F. Tassone, and F. Bassani, Solid State Commun. **77**, 641 (1991).
[5] J. Knoester, Phys. Rev. Lett. **68**, 654 (1992).
[6] J. Knoester, J. Lumin. **53**, 101 (1992).
[7] G. Björk, S. Pan, J. Jacobson, and Y. Yamamoto, Phys. Rev. B **50**, 17 336 (1994).

[8] G. Björk, S. Pan, J. Jacobson, H. Cao, and Y. Yamamoto, Phys. Rev. B **52**, 17 310 (1995).
[9] N.E. Rehler and J.H. Eberly, Phys. Rev. A **3**, 1735 (1971).
[10] T. Tokihiro, Y. Manabe, and E. Hanamura, Phys. Rev. B **47**, 2019 (1993).
[11] T. Tokihiro, Y. Manabe, and E. Hanamura, Phys. Rev. B **51**, 7655 (1995).
[12] E. Hanamura, J. Phys. Soc. Jpn. **37**, 1545 (1974); **37**, 1553 (1974).
[13] L.C. Andreani, Phys. Status Solidi B **188**, 29 (1995).
[14] P.W. Milonni, R.J. Cook, and J.R. Ackerhalt, Phys. Rev. A **40**, 3767 (1989).
[15] For example, see J.R. Ackerhalt and P.W. Milonni, J. Opt. Soc. Am. B **1**, 116 (1984); and *Photons and Atoms*, edited by C. Cohen-Tannoudgi, J. Dupont-Roc, and G. Grynberg (John Wiley & Sons, New York, 1989), pp. 293 and 307.
[16] K. Zaheer and M.S. Zubairy, Phys. Rev. A **37**, 1628 (1988).